MODERN AND ANCIENT EPEIRIC SEAS AND THE SUPER-ESTUARINE CIRCULATION MODEL OF MARINE ANOXIA

Thomas J. Algeo[1], Philip H. Heckel[2], J. Barry Maynard[1], Ronald C. Blakey[3] and Harry Rowe[4]

[1]Department of Geology, University of Cincinnati, Cincinnati, Ohio 45221-0013, U.S.A.; Thomas.Algeo@uc.edu
[2]Department of Geoscience, University of Iowa, Iowa City, Iowa 52242, U.S.A.
[3]Department of Geology, Northern Arizona University, Flagstaff, Arizona 86011, U.S.A.
[4]Department of Geological Sciences, University of Kentucky, Lexington, Kentucky 40506, U.S.A.

ABSTRACT

The boundary conditions and environmental characteristics conducive to widespread benthic anoxia in ancient epeiric seas are not well understood, in part due to a paucity of modern analogues. Three modern epicontinental seas (Hudson Bay, Baltic Sea and Gulf of Carpentaria) are examined with the goal of identifying key factors that contribute to the development of water-column stratification and deep-water oxygen depletion in such systems. The insights gained are applied to an analysis of the North American Late Pennsylvanian Mid-continent Sea (LPMS), an ancient epicontinental sea that developed sulfidic bottom-waters over a large area (~10^6 km^2) during a series of glacio-eustatic highstands. None of the modern epicontinental seas is a good analogue for the LPMS. The Gulf of Carpentaria, located at low latitudes in proximity to an active orogen subject to monsoonal precipitation, is closest to the LPMS in terms of geographic, tectonic and climatic boundary conditions, but its bottom-waters are well oxygenated owing to strong tidal mixing and anti-estuarine circulation. Hudson Bay is closest to the LPMS in terms of size, but diminished primary productivity at higher latitudes and lateral advection of oxygenated deep-waters inhibit development of benthic anoxia. The Baltic Sea is closest to the LPMS in terms of benthic redox conditions, with sulfidic bottom-waters over ~15% of its area, but its redox status is dependent on shallow marginal sills (<30 m) limiting deep-water renewal and on rates of primary productivity (120–240 g C m^{-2} y^{-1}) sufficient to deplete bottom-water of dissolved oxygen. By contrast, the LPMS seafloor was widely anoxic despite marginal sill(s) too deep (>100 m) to restrict renewal of the subpycnoclinal watermass and levels of primary productivity ($\leq$21 g C m^{-2} y^{-1}) insufficient to impose a high respiratory oxygen demand.

Although the LPMS shares certain important boundary conditions with the modern Baltic Sea (e.g., a humid climate and largely landlocked setting), while necessary were insufficient factors for the development of widespread

RESUME

On ne comprend bien ni les conditions des bordures ni les traits de l'environnement favorables à l'anoxie benthique générale dans des mers épicontinentales anciennes, en partie parce qu'il n'y a pas beaucoup d'analogues modernes. Ici on examine trois mers épicontinentales modernes (la Baie d'Hudson, la Mer Baltique et le Golfe de Carpentarie) avec le but d'identifier les facteurs principaux qui contribuent au développement de la stratification de colonnes d'eaux et à l'épuisement d'oxygène dans les eaux profondes de tels systèmes. Ensuite on applique les aperçus obtenus à une analyse de la Mer du Mid-Continent de l'Amérique du Nord du Pennsylvanien Supérieur (LPMS), une mer épicontinentale ancienne qui a développé des eaux de fond sulfidiques à travers une grande étendue (10 km) durant une série de périodes de hautes eaux glacio-eustatiques. Aucune des mers épicontinentales modernes n'est un bon analogue pour la LPMS. Le Golfe de Carpentarie, qui se trouve à des latitudes basses près d'une orogène active exposée à la précipitation de moussons, ressemble le plus à la LPMS quant aux conditions de bordures géographiques, tectoniques et climatiques; mais ses eaux de fond sont bien oxygénées à cause d'un fort mélange de marées et d'une circulation anti-estuarine. La Baie d'Hudson ressemble le plus à la LPMS quant à son volume; mais la productivité primaire diminuée à de plus hautes latitudes et l'avection latérale d'eaux profondes oxygénées empêchent le développement d'anoxie benthique. La Mer Baltique ressemble le plus à la LPMS quant aux conditions rédox benthiques avec des eaux sulfidiques à travers ~15 % de son étendue; mais son rédox dépend de seuils marginaux peu profonds (<30 m) qui limitent le renouvellement d'eaux profondes, et de taux de productivité primaire (120–240 g C m^{-2} y^{-1}), suffisants pour épuiser l'oxygène dissolu dans les eaux du fond. Par contraste, le fond de la mer de la LPMS était largement anoxique malgré des seuils marginaux trop profond (>100 m) pour empêcher benthic anoxia in the LPMS. A critical boundary condition unique to the LPMS was the preconditioned, oxygen-deficient character of the intermediate watermass that was laterally advected into this sea. The redox status of these waters was a consequence of: (1) a marked shallowing of the oxygen-minimum zone in the eastern Panthalassic Ocean, near the entrance of the corridor leading to the LPMS; and (2) watermass aging during its traverse through the ~1000 km long Greater Permian Basin Seaway leading to the LPMS. Large-scale, estuarine-type circulation in combination with lateral advection of oxygen-deficient intermediate waters are thus key features of the *super-estuarine circulation model* for development of epicontinental marine anoxia, which is typified by the LPMS but distinct from widely cited silled basin and upwelling-zone models for marine anoxia. Because the benthic redox status of the LPMS was dependent on the strength and lateral extent of its halocline and, hence, on freshwater discharge into the sea, the system was highly sensitive to climate fluctuations at intermediate time scales (i.e., hundreds to tens of thousands of years.

niveaux de productivité primaire ($\leq$21 g C $m^{-2}y^{-1}$) insuffisants pour imposer une haute demande d'oxygène respiratoire.

Bien que la LPMS partage quelques conditions de bordure importantes avec la Mer Baltique moderne (e.g., un climat humide et un site pour la plupart entouré de terre), ces conditions, quoique nécessaires, étaient des facteurs insuffisants pour le développement de beaucoup d'anoxie benthique dans la LPMS. Une condition de bordure critique, qui est unique à la LPMS, était la qualité 'préconditionnée' d'une manque d'oxygène dans la masse d'eau intermédiaire qui a été avectée latéralement dans cette mer. Le rédox de ces eaux s'est développé parce que: (1) la zone d'oxygène minimum dans l'Océan Panthalassique de l'est, près de l'entrée du couloir menant à la LPMS, est devenue beaucoup peu profonde; et (2) la masse d'eau s'est vieillie pendant son voyage de ~1000 km dans la Route de la Mer du Bassin du Permien Supérieur qui menait à la LPMS. Une grande circulation du type estuarien combinée avec de l'avection latérale d'eaux intermédiaires dépourvues d'oxygène sont ainsi des traits importants du *modèle de circulation super-estuarienne* pour le développement d'anoxie marine épicontinentale, ce qui est typifié par la LPMS mais distincte de modèles de zones d'upwelling et de bassin à seuils souvent cités pour l'anoxie marine. Parce que le rédox benthique de la LPMS dépendait de la force et de l'étendue latérale de son halocline et, par conséquent, de l'épanchement d'eau douce dans la mer, le système était bien sensible à des fluctuations de climat aux échelles de temps intermédiaires (i.e. des centaines à des dizaines de milliers d'années).

INTRODUCTION

Anoxic facies were widely developed on the North American craton during the Late Pennsylvanian and other epochs, yet the modern world offers few if any good analogues for the environments in which these organic-rich sediments accumulated. Most epicontinental seas, such as Hudson Bay and the Gulf of Carpentaria, are characterized by oxic to suboxic seafloor conditions. Recent anoxic marine environments are mostly located in oceanic or continental margin settings and classified either as silled basins, such as the Black Sea, Cariaco Trench, and Santa Barbara Basin, or as continental margin upwelling zones, such as the Peru Shelf, the Namibian Shelf, and the Arabian Sea (e.g., Demaison and Moore, 1980; Wignall, 1994; Arthur and Sageman, 1994; Hay, 1995). The only example of a modern epicontinental sea subject to widespread anoxia is the Baltic Sea, in which benthic oxygen depletion is due to a combination of hydrographic restriction and strong estuarine circulation, characteristics shared with many anoxic fjords. The paucity of modern analogues for anoxic paleoenvironments in epicontinental settings is a major factor limiting the understanding of the environmental conditions and dynamics responsible for formation of many ancient black shales.

The goal of this paper is to review the boundary conditions and environments of large modern epicontinental seas, with a focus on the relationship of hydrologic, bathymetric, hydrographic and productivity factors to benthic redox conditions, and to apply the insights thus gained to an analysis of the Late Pennsylvanian Mid-continent Sea (LPMS). Three modern seas were chosen: (1) Hudson Bay, the largest modern epicontinental sea (1.23 x 10^6 km^2) and the closest to the LPMS in size; (2) the Baltic Sea, the only modern epicontinental sea exhibiting widespread seafloor anoxia and, thus, the most similar to the LPMS in terms of benthic redox conditions; and (3) the Gulf of Carpentaria, the modern epicontinental sea that most closely matches the geographic, climatic and tectonic boundary conditions of the LPMS. As discussed herein, none of these modern seas is a good analogue for the LPMS, in which development of widespread benthic anoxia appears to have depended on a unique combination of factors, that is strong precipitation and fluvial discharge in a periequatorial setting, large-scale estuarine-type circulation within a broad, mostly shallow and geographically restricted epicontinental sea, and lateral advection of preconditioned, oxygen-deficient intermediate waters from below an oceanic thermocline. Because the

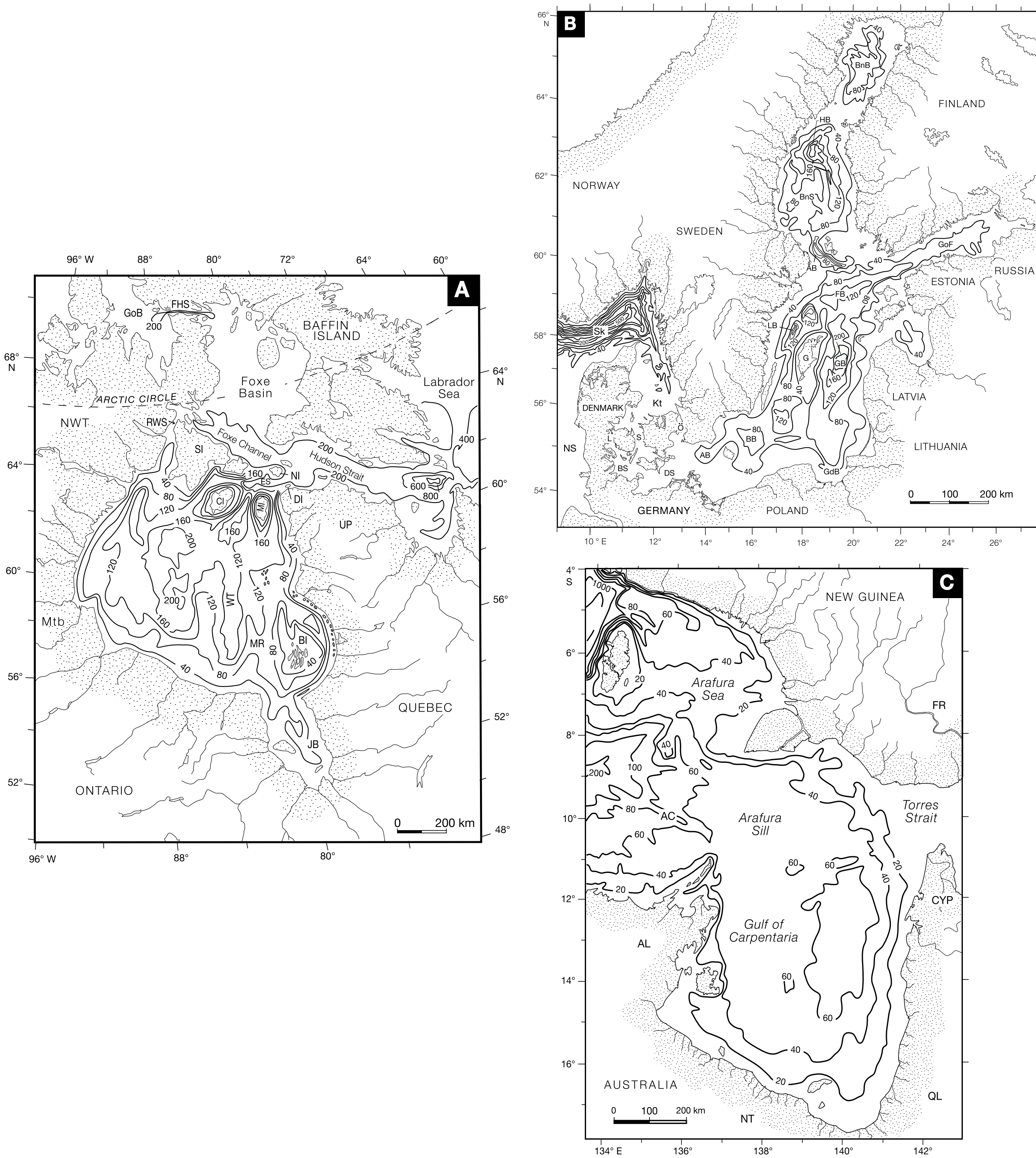

Figure 1. Maps of modern epicontinental seas: (A) Hudson Bay, (B) Baltic Sea and (C) Gulf of Carpentaria. Bathymetric contours shown in A and B at 40 m intervals (to 200 m) and 100 m intervals (below 200 m), and in C at 20 m intervals (to 100 m; irregular intervals below this depth). Abbreviations: (A) BI = Belcher Islands, CI = Coates Island, DI = Digges Island, ES = Evans Strait, FHS = Fury and Hecla Strait, GoB = Gulf of Boothia, JB = James Bay, MI = Mansel Island, MR = Mansel Ridge, Mtb = Manitoba, NI = Nottingham Island, NWT = Northwest Territories, RWS = Roes Welcome Strait, SI = Southampton Island, UP = Ungava Peninsula, WT = Winisk Trough; (B) AB = Arkona Basin, ÅB = Åland Basin, BB = Bornholm Basin, BnB = Bothnian Bay, BnS = Bothnian Sea, BS = Belt Sea, DS = Darss Sill, FB = Fåro Basin, G = Gotland, GB = Gotland Basin, GdB = Gdansk Basin, GoF = Gulf of Finland, HB = Harnosand Basin, Kt = Kattegat, L = Lillebælt, LB = Landsort Basin, NS = North Sea, Ö = Ö ælt, Sk = Skagerrak; (C) AC = Arafura Channel, AL = Arnhem Land, CYP = Cape York Peninsula, FR = Fly River, NT = Northern Territory, QL = Queensland.

Table 1. Comparative statistics for modern and ancient epicontinental seas.

	Hudson Bay	Baltic Sea	Gulf of Carpentaria	Late Pennsylvanian Mid-continent Sea[+]
Area (10^3 km^2)	1230	420	510	2100
Average depth (m)	120	55	40	~50
Volume (10^3 km^3)	160	21.5	20.4	~105
Freshwater discharge (km^3 y^{-1})	975	485	230	~800–1500
Volume:discharge ratio (y)	130	45	90	~70–130
Surface circulation	cyclonic	cyclonic	variable	cyclonic
Sill depth (m)	~200	18	53	>100
Deep-water renewal rate (10^6 m^3 s^{-1})	~0.2	0–0.2	n/a	~0.1–0.2
Deep-water renewal pattern	continuous	episodic (1–20 y)	n/a	continuous
Dissolved O_2 of source deep-water (% saturation)	>60	>80	n/a	<50
Tidal regime[†]	micro to meso	micro	meso to macro	micro
Halocline depth (m)	15–30	40–80	none*	15–30
2° pycnocline (m)	none	110–150	none	none (?)
Subpycnoclinal volume: total basin volume (%)	>80	~25	n/a	50–75
Shallow σ_t, deep σ_t[‡]	20–24, 26–27	4–6, 8–10	22–23, 23–25	23–27, 34–38
$\Delta\sigma_t$ (deep-shallow)[‡]	~4.5	~4	~1.5	11 ± 4
Primary productivity (g C m^2 y^{-1})	<30–100	120–240	200–670	≤21[a]
Sediment TOC (wt%)	<1 (~3)	3–8 (~20)	n.d.	5–30
C_{org} burial flux[§] (g C m^2 y^{-1})	~1	12–32	n.d.	≤2.1
Preservation efficiency (%)[b]	~2	~10	n.d.	>10
Spatial pattern of benthic redox variation	none	basin-centred	none	lateral gradient

[†] Microtidal = <2 m tidal range, mesotidal = 2–4 m, and macrotidal = >4 m.

* A seasonal thermocline develops at a depth of 30–40 m.

[‡] σ_t is calculated as watermass density in units of kg m^3 minus 1000.

[§] Based on average Holocene sedimentation rates of ~1 mm y^1, characteristic of the central areas of both the Baltic Sea and Hudson Bay (Leslie, 1964; Winterhalter et al., 1981; Emeis et al., 1992), and a dry bulk density of ~400 kg m^3 (e.g., Biksham and d'Anglejan, 1989).

[+] n/a = not applicable; n.d. = not determined or data unavailable.

[a] Estimated maximum C_{org} sinking flux (median estimate is ~1 g C m^2 y^1).

[b] Calculated as the ratio of C_{org} burial flux to primary productivity; note that the same term is used for the ratio of C_{org} burial flux to organic C sinking flux (e.g., Canfield, 1994).

main factors that controlled development of benthic anoxia in the LPMS are conceptually distinct from those responsible for anoxia in silled-basin and upwelling-zone systems, we propose a new model for epicontinental marine anoxia, the *super estuarine circulation model*, for which the LPMS may be considered the type example. The super-estuarine circulation model may be relevant to other ancient epicontinental seas characterized by widespread benthic anoxia.

MODERN EPICONTINENTAL SEAS

HUDSON BAY

Hudson Bay, the largest modern epicontinental sea, has an area of 1.23 x 10^6 km^2 and a volume of 160 x 10^3 km^3, including James Bay, a large embayment at its southern end (Fig. 1A; Table 1). It occupies a geologically ancient depression that was repeatedly depressed by the mass of Pleistocene icesheets and that continues to isostatically rebound today, albeit at a comparatively slow rate (Mitrovica et al., 2000). It is saucer-shaped, with an average water depth of ~120 m and a maximum depth of ~325 m (Pelletier, 1986), but divided into several subbasins by shallow, North–South-trending submarine ridges (Norris, 1993). It connects to the Arctic Ocean through an intricate northern waterway (including the Foxe Basin, Fury and Hecla straits, and the Gulf of Boothia) and to the Labrador Sea to the east through Hudson Strait. Ingress of Arctic waters is severely constrained by the ~25 km wide, <50 m deep Roes Welcome Strait, whereas deep-water exchange with the Labrador Sea through the ~300 km wide, ~200 m deep Evans Strait (at the western end of Hudson Strait) is comparatively uninhibited (Fig. 2A; Drinkwater, 1986).

Both Hudson Bay and Hudson Strait exhibit estuarine circulation, with inflow of more saline deep-waters and outflow of less saline surface-waters. The deep water that is recharged through Hudson Strait is ultimately drawn mainly from Arctic surface-waters with only a minor component of

These waters, which are tidally mixed in Hudson Strait before entering Hudson Bay, are slightly oxygen-depleted (~85% of surface saturation levels). Export of Hudson Bay waters through Hudson Strait varies seasonally in the range of ~0.1–0.3 x 10^6 m^3 s^{-1} (Campbell, 1958; Collin, 1966; Drinkwater, 1986; Goldstein and Jacobsen, 1988). Because freshwater discharge into Hudson Bay is comparatively small (975 km^3 y^{-1}, or 0.03 x 10^6 m^3 s^{-1}), the deep-water influx into Hudson Bay is nearly as large as total outflow, that is, ~0.07–0.27 x 10^6 m^3 s^{-1} (Table 1). The Arctic connection through the narrow (~16 km wide) Fury and Hecla Strait has a lower flux, <0.1 x 10^6 m^3 s^{-1} (Collin, 1966).

Hudson Bay has a drainage basin of 5.8 x 10^6 km^2 fed by hundreds of rivers, of which the largest are the Nelson and Churchill feeding directly into Hudson Bay, and the LaGrande and Albany feeding into James Bay. The total mean annual discharge is 30,900 m^3 s^{-1}, or 975 km^3 y^{-1} (Hydrological Atlas of Canada, 1978), equivalent to ~0.6% of the total volume of the bay (Table 1). Hudson Bay is seasonally ice-covered, and ice rafting is a significant process in sediment transport within the bay (Pelletier, 1986). Freshwater discharge into the bay peaks during the summer when the ice cover disintegrates (Tomczak and Godfrey, 1994). Surface currents in Hudson Bay follow a cyclonic (counter clockwise) gyre, although there is a strong overall northward component to flow during the late summer and fall as the freshwater influx peaks. Hudson Bay is micro- to mesotidal with semi-diurnal tidal ranges of ~10 cm along the eastern margin increasing to ~125 cm along the western margin with tidal ranges as large as 3–5 m locally in bays (Collin, 1966; Prinsenberg and Freeman, 1986). Tidal currents are relatively strong in the vicinity of Evans Strait, reaching velocities of >2.0 m s^{-1}.

The Hudson Bay watermass is stratified with a pycnocline (thermohalocline) at a depth of 15–30 m; annual mixing is limited to a depth of ~60 m (Pett and Roff, 1982). The shallowness of the pycnocline results in the deep-watermass accounting for >80 % of the total volume of the bay (Fig. 2A; Table 1). Surface-waters are slightly warmer and less saline (5–10°C; 25–30‰) than deep-waters (<0°C; ~33‰), although density differences across the pycnocline are relatively small (σ_t = 20–24 for surface-waters and σ_t = 26.5 for deep-waters; Barber, 1968; Prinsenberg, 1986). Based on sparse data, dissolved oxygen levels in deep-waters are mostly >60% of surface saturation levels with some observations as low as 34%, indicating oxic to weakly suboxic seafloor conditions; however, an abundant and diverse benthic biota is present throughout the bay (Pelletier et al., 1968; Pett and Roff, 1982). Vertical mixing rates are moderate, with deep-water renewal at timescales of ~3–5 years near the northern straits and ~4–14 years elsewhere in the basin (Pett and Roff, 1982; Prinsenberg, 1986). Cyclonic deep-water circulation within Hudson Bay results in older waters in the central and southeastern parts of the bay; westerly winds on the western margin of the bay contribute also to greater vertical mixing there (Maxwell, 1986). The degree of water-column stratification varies seasonally, intensifying during the summer and fall owing to increased freshwater discharge.

Primary productivity is greatest around the margins of the bay (~70–100 g C m^{-2} y^{-1}), owing to both riverine nutrients and vertical mixing with nutrient-rich bottom-water (Table 1; Anderson and Roff, 1980; Prinsenberg, 1986; Roff and Legendre, 1986). By contrast, the centre of the bay exhibits lower levels of productivity (<30 g C m^{-2} y^{-1}). Stratification contributes to low productivity in the centre of the basin through sequestering of nutrients in the deep-water layer. Factors that limit the overall productivity of the bay include its winter ice cover, low light levels (especially in the spring and fall) resulting from its high latitude, and low rates of nitrogen regeneration in the deep-watermass (Anderson and Roff, 1980; Pett and Roff, 1982). The sediments are mostly calcareous clays and silty clays with an average $CaCO_3$ content of 20–30%; much of the sediment is of Pleistocene glacial erosive origin and reflects the lithology of the underlying bedrock (Pelletier, 1986). Maximum TOC values are 2–3%, associated mainly with channel sediments in the north and a few areas of fine-grained sedimentation in the basin interior and southeast (Pelletier et al., 1968; Pelletier, 1986; Biksham and d'Anglejan, 1989); however, about 95% of the bay area has sediments with <1% TOC, averaging ~0.25%. Sediment discharge into Hudson Bay is relatively high owing to the availability of large quantities of glacial sediment; ice-rafted deposits are concentrated along the western and southwestern bay margins (Martini, 1986; Pelletier, 1986). Deep-water sediments are mostly grey-green to reddish-brown muds and silty muds, reflecting varying redox conditions, with locally reducing microenvironments yielding black muds (Leslie,

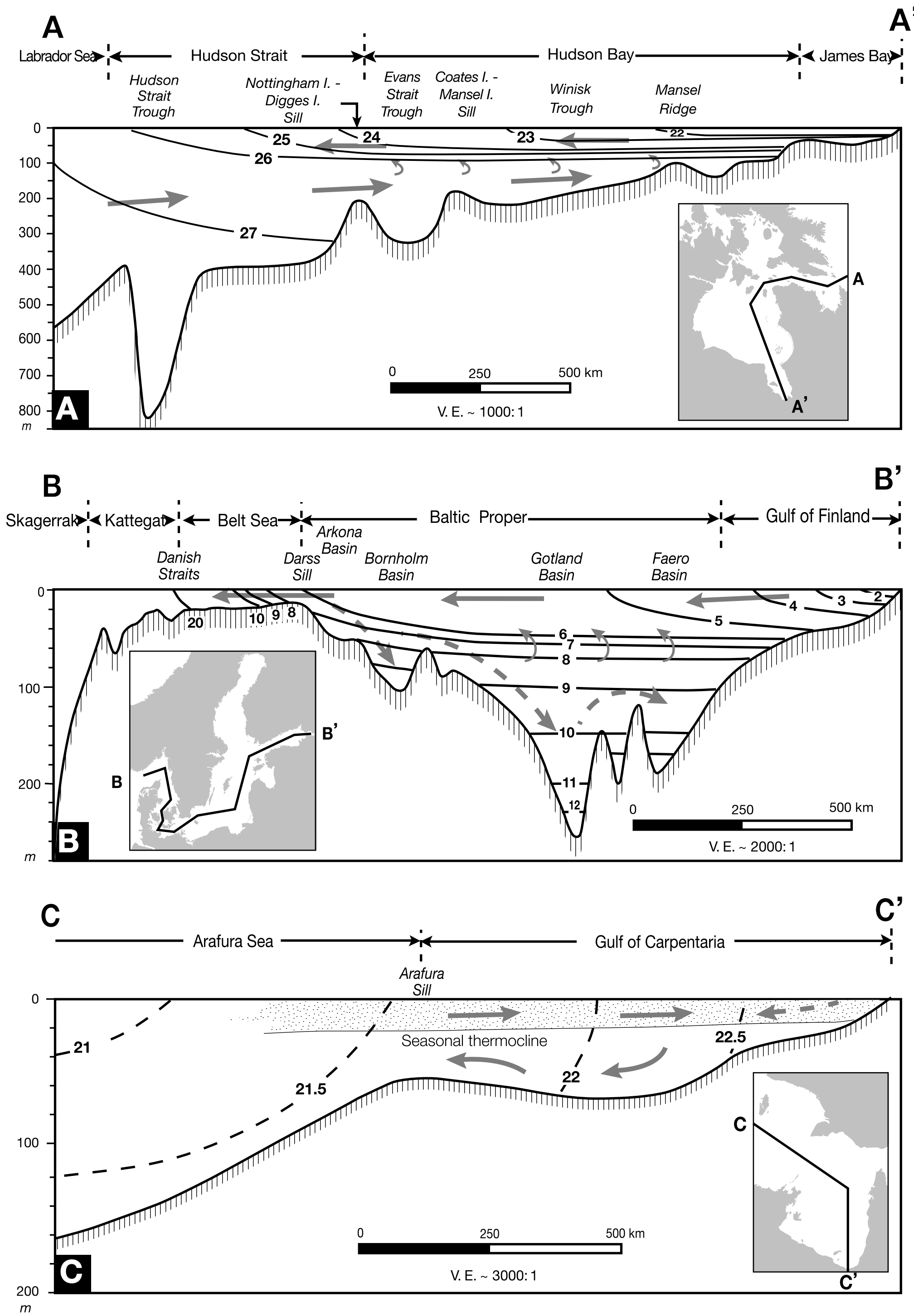

Figure 2. Cross-sections of modern epicontinental seas: (A) Hudson Bay, (B) Baltic Sea and (C) Gulf of Carpentaria. Watermass isopycnals represent contoured σ_t values (i.e., watermass density in kg m^{-3} minus 1000) calculated from the international equation of state of seawater (UNESCO, 1981, as given in Chester, 1990) using temperature–salinity data in Rochford (1966), Newell (1973), Kullenberg (1981), Forbes (1984), Drinkwater (1986), Prinsenberg (1986), Winkel-Steinberg et al. (1992), Rothlisberg et al. (1994) and HELCOM (1996). Watermass circulation patterns are shown by arrows; broken arrows in B indicate episodic deep-water influx into the Baltic Sea, and broken arrows in C indicate seasonal (i.e., monsoonal) discharge into the Gulf of Carpentaria. Watermass conditions within the Danish Straits can be highly variable depending on local meteorological conditions and Baltic outflow rate (Winkel-Steinberg et al., 1992). Watermass density and circulation patterns within the Gulf of Carpentaria can vary seasonally (Forbes, 1984); C represents average interannual conditions. Note differences in horizontal and vertical scales between panels.

1964; Pelletier, 1986). The thickness of the Holocene sediment cover is only approximately known; thicknesses of 3–7 m may be typical, with accumulations to 20 m or more in topographic depressions (Leslie, 1964).

THE BALTIC SEA

The Baltic Sea is an epicontinental sea with an area of 0.42 x 10^6 km^2 and a volume of 21.5 x 10^3 km^3 (Fig. 1B; Table 1). It consists of a large central area (the Baltic proper) and several adjoining gulfs and bays, the largest of which are the Bothnian Sea, Bothnian Bay and Gulf of Finland. It is mostly shallow with a mean depth of 55 m but contains a series of topographic depressions separated by sills (Glasby et al., 1997). From its exterior (oceanward) to its interior (cratonward) margin, these depressions include the Arkona (55 m maximum depth), Bornholm (105 m), Gdansk (116 m), Gotland (249 m), Landsort (459 m) and Fåro (208 m) basins in the Baltic proper, and the Åland (290 m) and Harnosand basins (230 m) in the Bothnian Sea (Fig. 2B). However, areas >100 m deep occupy less than 5% of the area of the Baltic Sea, whereas shoals with depths <20 m occupy broad areas, especially in the southern Baltic (Fig. 1B).

The Baltic Sea is connected to the North Sea through the Danish Straits and thence through the Kattegat and Skagerrak (Fig. 1B). The Danish Straits were shaped as fluvial valleys during the Late Weichselian and Early Holocene when eustatic elevations were lower than at present (Björck, 1995; Andrén et al., 2000). The main straits are the Öresund, which connects directly to the western part of the Baltic, and the Storebælt and Lillebælt, which connect to the Baltic via the Belt Sea and the 18 m deep Darss Sill (Lemke and Kuijpers, 1995; Lemke et al., 2001). These straits strongly attenuate tidal energy, resulting in a microtidal range (<20 cm) in the Baltic Sea (Alhonen, 1966). Winds induce somewhat larger variations in sea-level elevation through the straits, to ~0.5 m and, hence, surface circulation and mixing of surface-waters are mainly wind-controlled.

The Baltic Sea has a large positive water balance owing to strong fluvial discharge and low evaporation and, hence, exhibits an estuarine circulation pattern (Ehlin, 1981; Kullenberg, 1981; HELCOM, 1996). The drainage basins of ~250 tributary rivers cover an area that is four times that of the sea itself, and the annual discharge of 420–550 km^3 (~13,300–17,400 m^3 s^{-1}) is equivalent to ~2% of the volume of the Baltic Sea basin (Table 1). The Baltic watermass is brackish due to restricted inflow of waters of near-normal marine salinity through the Danish Straits. At present, Storebælt carries ~75% of the brackish surface-water outflow from the Baltic and almost all of the more saline deep-water influx, which is drawn from surface-waters of the North Sea via the Skagerrak and Kattegat (Segerstråle, 1957). The deep-water influx averaged over longer intervals is about the same magnitude as fluvial discharge into the Baltic (Ehlin, 1981; HELCOM, 1996; Lass and Matthäus, 1996).

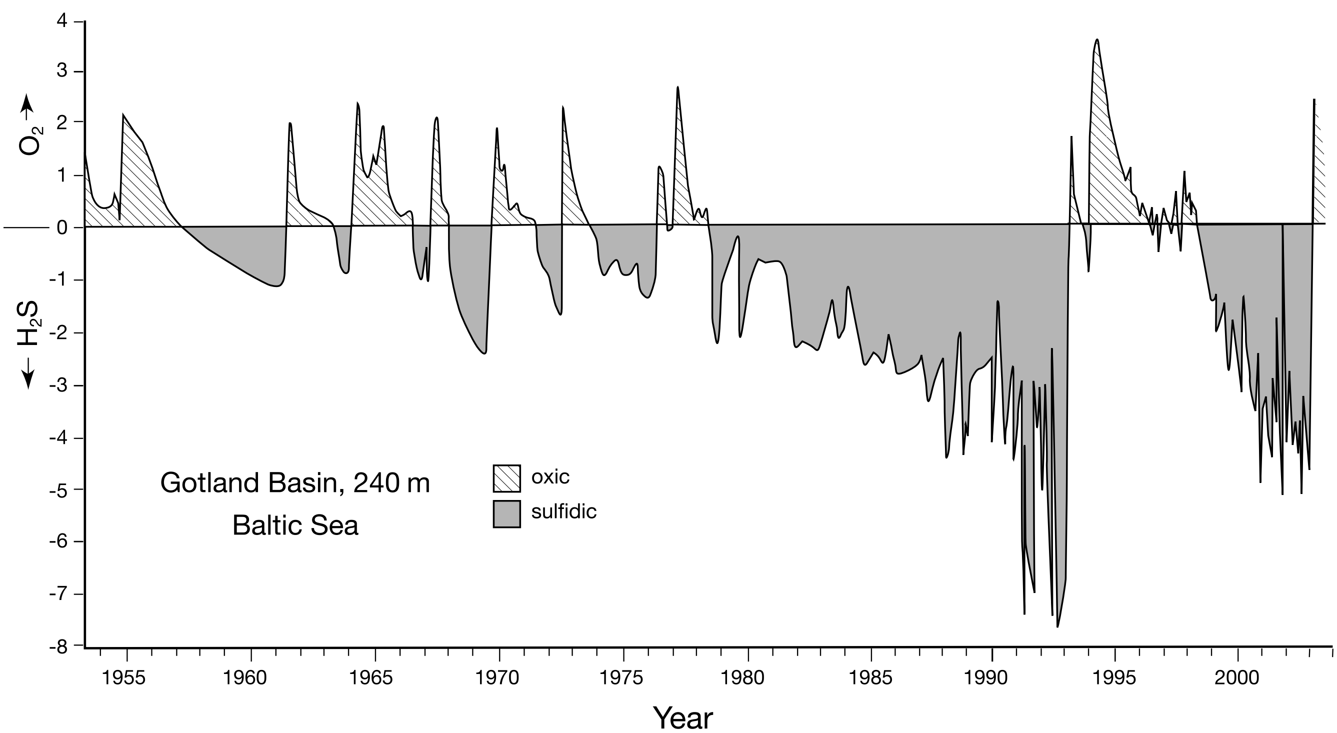

Figure 3. Temporal variation in the redox conditions of Baltic seawater in the deep Gotland Basin (240 m). H_2S values given as negative O_2 equivalent. Data from Grasshoff and Voipio (1981), Matthäus (1995) and Nausch et al. (2003).

However, deep-water recharge is highly episodic, requiring an unusual combination of wind shifts to force saline waters from the Kattegat over the Danish Straits and into the Baltic proper. These events are typically rapid (~0.2 x 10^6 m^3 s^{-1}) but of short duration (1–10 days; Lass and Matthäus, 1996). Deep-water recharge has recurred historically at intervals of one to a few years, but the period from 1978 to 1993 was exceptional in lacking such events (Fig. 3; Matthäus, 1995; Nausch et al., 2003).

As a consequence of these topographic and hydrographic factors, the Baltic Sea exhibits a strong gradient in water chemistry from the exterior regions, which are brackish, to the interior regions, which are nearly fresh (Fig. 2B; Segerstråle, 1957; Glasby et al., 1997). Salinities change rapidly through the Danish Straits, from ~30‰ in the Kattegat on the oceanward side to <10‰ in the Arkona Sea on the cratonward side. The Baltic proper has a surface-water salinity of ~7–8‰, but this falls sharply to values <3 ‰ in the interior regions (i.e., the Bothnian Sea and Gulf of Finland). Deep-waters are 5–15‰ more saline than overlying surface-waters in the Belt Sea and Arkona Basin proximal to the Danish Straits, but the deep-to-shallow differential diminishes to <1 ‰ in the interior regions. Temperatures, though strongly seasonal, range up to 15°C in surface-waters but are generally <4°C in the deep-watermass. Typical densities (σ_t) for surface and deep-waters of the Baltic proper are ~4–6 and ~8–10, respectively (Table 1).

A seasonal thermocline develops within the surface-watermass at a depth of ~20–30 m and a permanent pycnocline (halocline) separates surface-waters from denser deep-waters in the Baltic Sea (Kullenberg, 1981; Glasby et al., 1997). The depth of the halocline increases northeastward across the Baltic as the volume of brackish surface outflow increases relative to that of the saline deep inflow. Thus, the halocline is found at 30–40 m in the Arkona Basin, 40–50 m in the Bornholm Basin, and 60–80 m in the Gotland and Landsort basins (Fig. 2B), and the subpycnoclinal watermass accounts for only about ~25% of the volume of the Baltic proper (Table 1). The halocline is weak or absent in the interior gulfs owing to shallowing of the seafloor and enhanced upwelling. In some of the deeper basins, a secondary pycnocline (halocline) is present at depths of ~100–120 m; many recharge events fail to penetrate this pycnocline, limiting renewal to the intermediate watermass (Grasshoff and Voipio, 1981).

Although the surface-watermass is well-oxygenated (6–8 mL L^{-1}), dissolved O_2 levels decline sharply below the pycnocline to values <1 mL L^{-1} (Matthäus, 1995; HELCOM, 1996; Nausch et al., 2003). Redox conditions are sufficiently oxygen-depleted as to exclude benthic fauna within stagnant bathymetric depressions with a total area of ~70,000 km^2, or ~15% of the Baltic proper (HELCOM, 1996). Whereas the exterior basins such as the Arkona and Bornholm deeps are characterized by suboxic, nonsulfidic bottom-water, H_2S is present in deep-waters of the Gotland Basin (Matthäus, 1995). This is a consequence of the irregular seafloor bathymetry of the Baltic, which causes recharging deep-waters to collect in the exterior basins and to advance only slowly cratonward (Fig. 2B; Sohlenius et al., 2001). Whereas the dissolved oxygen content of hyperpycnal waters entering the Danish Straits is typically near saturation, it is commonly reduced to 2–3 mL L^{-1} by the time that recharging watermasses reach the Gotland Deep (Grasshoff and Voipio, 1981). Benthic oxygen depletion appears to have intensified in recent decades due to a combination of higher productivity associated with anthropogenic nutrient loading and climatic warming (Dybern and Fonselius, 1981; Karhu et al., 1994; Matthäus, 1995; HELCOM, 1996; Nausch et al., 2003) and changes in regional wind patterns that influenced rates of deep-water recharge (Lass and Matthäus, 1996). However, geological evidence indicates that the Baltic is also subject to natural climate-related fluctuations in benthic redox conditions at longer time scales (Matthäus, 1995).

Primary productivity is comparatively low in the interior regions (*e.g.*, 25–50 g C m^{-2} y^{-1} in Bothnian Bay) compared with the Baltic proper (120–240 g C m^{-2} y^{-1}; Table 1; Hällfors et al., 1981). However, episodic upwelling events, as in the Gulf of Finland in 1969, bring P-rich deep-waters into the photic zone, stimulating phytoplankton blooms especially of nitrifying cyanobacteria (Niemi, 1979; Wasmund, 1997). Sediment TOC content is spatially variable but mostly 3–8% (Sternbeck and Sohlenius, 1997; Andrén et al., 2000; Sohlenius et al., 2001). TOC is related to benthic redox conditions: areas overlain by waters with low but measurable O_2 concentrations accumulate bioturbated green-grey, weakly organic muds (gyttjas), whereas areas with sulfidic bottom-water accumulate laminated black, organic-rich muds (sapropels; Manheim, 1961). Redox-sensitive trace elements such as Mo, U, Cu and Zn exhibit a strong association with the latter. The recent intensification of benthic anoxia has resulted in an increase in the area of deposition of laminated, organic-rich sediments (Larsson et al., 1985; Jonsson et al., 1990; Struck et al., 2000).

The Baltic has a complex history of variation in size, depth and environmental characteristics during the late Pleistocene. It was transformed from a freshwater lake to a brackish marginal marine body beginning ~10.1 ky B.P. and accelerating ~8 ky B.P. in response to sea-level rise and sill deepening (Andrén , 2000; Sohlenius et al., 2001). Deposition of laminated, organic-rich sediments began in the deepest portions of the most distal basins and spread to shallower depths and more proximal locations as denser, saline waters accumulated in topographic depressions and locally strengthened the pycnocline (Sohlenius et al., 2001). An abrupt increase in organic carbon content is observed at the "Initial Littorina/Littorina Sea" transition (~7.8 ky B.P.) throughout the Baltic basin and is most likely due to increased primary production in response to increased nutrient availability, following an incursion of nutrient-rich seawater and/or enhanced chemical weathering associated with a warmer climate (Sohlenius and Westman, 1998; Andrén et al., 2000). The increase is associated with a transition from P-limited to N-limited conditions and consequent blooms of N-fixing cyanobacteria (Bianchi et al., 2000).

THE GULF OF CARPENTARIA

The Gulf of Carpentaria, with an area of 0.51 x 10^6 km^2, is located in a large embayment on the northern Australian continental margin (Fig. 1C; Edgar et al., 2003). It is bordered by the narrow coastal plains and peri equatorial Central Ranges of New Guinea to the north and by the low lying Australian craton to the south, thus ranging in latitude from 4°S to 18°S and spanning climate zones from humid tropical to dry tropical. The gulf has a shallow, relatively featureless seafloor, with average and maximum depths of 40 m and 69 m, respectively (Torgersen et al., 1983). To the northwest, it communicates with the Arafura Sea across the ~100 km wide Arafura Sill, which is 53 m deep and exhibits only ~2 m of relief (Fig. 2C). The Arafura Sea, ~0.72 x 10^6 km^2 in area, is mostly <80 m deep; however, its southwestern quadrant is deeper (to ~200 m) owing to incision by lowstand river systems, and is open to the Indian Ocean on the west along a ~1000 km long shelf margin (Jongsma, 1974; Jones and Torgersen, 1988; Torgersen et al., 1988; Edgar et al., 2003). To the northeast, the Gulf of Carpentaria communicates with the Coral Sea via Torres Strait, a wide (120 km) but shallow (5–18 m) passage that is ~70% occluded by coral reefs and islands (Fig. 1C; Jennings, 1972; Wolanski, 1992). Channels through this strait are narrow and subject to strong currents $^{-1}$) driven by sea-level elevation differences up to 0.6 m.

The Gulf of Carpentaria has a monsoonal climate with strongly seasonal precipitation (Edgar et al., 2003). Dry southeast winds prevail during much of the year, with rainfall associated with northwesterly winds during the southern hemisphere summer (December–March). The drainage basins of tributary rivers to the gulf have an area of 1.22 x 10^6 km^2, located mostly (>90%) in northern Australia; however, ~80% of fluvial discharge comes from the wetter New Guinea landmass. Precipitation in New Guinea averages ~200–300 cm y^{-1} (Ludwig and Probst, 1998; Cecil et al., 2003a) whereas the drier northern Australian coast receives ~15–20 cm y^{-1} and the continental interior even less (Torgersen et al., 1988). Total annual discharge into the Gulf of Carpentaria is ~230 km^3 (Table 1), but it may have been as much as 700 km^3 y^{-1} prior to the Late Quaternary diversion of New Guinea's Fly River (Torgersen et al., 1988). The Fly River, which now debouches into the Gulf of Papua east of Torres Strait, has a discharge (470 km^3 y^{-1}) sufficient to create a brackish (15–30‰ S) surface-water plume to a depth of ~15 m that is detectable up to ~200 km offshore (Wolanski, 1992).

Despite its apparent geographic restriction, waters in the Gulf of Carpentaria are only minimally modified relative to normal seawater: surface-waters average 29–30°C and 35–36‰ salinity, and deep-waters are cooler (24–26°C) and of similar salinity (Forbes, 1984; Wolanski and Ridd, 1990; Somers and Long, 1994). A thermocline is present at ~30–40 m water depth during the summer, and a lateral salinity gradient of ~1‰ exists with more saline waters located in the southern gulf, proximal to the Australian coast (Fig. 2C). The summer monsoon results in a slight intensification of water-column stratification through warming of surface-waters and enhanced fluvial discharge. However, several factors prevent development of a permanent halocline in the Gulf of Carpentaria: (1) the more enclosed southern end of the gulf has a negative water balance owing to limited freshwater discharge from the Australian craton, promoting anti-estuarine circulation; and (2) the more open northern end of the gulf is subject to strong vertical mixing associated with tidal currents through Torres Strait (Forbes, 1984; Wolanski and Ridd, 1990; Somers and Long, 1994; Porter-Smith et al., 2004). Bottom-water are generally well oxygenated and support an abundant and moderately diverse benthic biota (Long and Poiner, 1994), although dissolved O_2 can be reduced to 30–50% of surface levels in the central part of the gulf during the summer months (Forbes, 1984).

The Gulf of Carpentaria is underlain by a depositional basin containing 1500–4000 m of predominantly Jurassic to Recent sediment, delimited by structural highs beneath the Arafura Sill and Torres Strait (Jennings, 1972; Jongsma, 1974; Doutch, 1976; Edgar et al., 2003). The Plio-Pleistocene section records at least 14 basinwide glacioeustatic transgressive–regressive cycles, broadly comparable to Late Pennsylvanian cyclothems of the North American mid-continent (Edgar et al., 2003). During the Late Pleistocene (~40 to 13 ky), the gulf was probably a freshwater lake; when global sea level rose above the 53 m depth of the Arafura Sill, it initially went brackish and then fully marine by ~10 ky (Torgersen et al., 1983, 1988; De Deckker et al., 1988). Benthic conditions were episodically anoxic during the lacustrine interval, resulting in deposition of laminated dark grey muds, but the Holocene marine sediments are grey-green sandy and shelly muds and muddy sands, fining toward the basin centre and locally along sheltered portions of the western basin margin (Jones, 1987; De Deckker et al., 1988; Torgersen et al., 1988). TOC contents are unreported and but presumably low. Approximately 80 cm of sediment has been deposited since 13 ky at an average rate of <0.1 mm y^{-1}. Primary productivity rates are very high in nearshore areas (~370–670 g C m^{-2} y^{-1}) and moderately high in offshore areas (~200–280 g C m^{-2} y^{-1}; Table 1; Rothlisberg et al., 1994).

THE LATE PENNSYLVANIAN MID-CONTINENT SEA

During the Middle Pennsylvanian to Early Permian, the North American craton was repeatedly flooded by glacio-eustatic transgressions, episodically forming a broad epicontinental sea. In the mid-continent region, these transgressions resulted in deposition of 3–10 m thick stratal packages or "cyclothems" (Heckel, 1977, 1980, 1991, 1994). In Iowa, Illinois and Indiana, such packages are coal-bearing and capped by paleosols, whereas in southeastern Kansas and northern Oklahoma, cyclothems consist mainly of marine shales and limestones and may lack a paleosol cap. The deepest water facies of cyclothems are the core shales, <1 m thick layers of laminated, grey to black, organic-rich sediments that accumulated under anoxic conditions. Core shales (so-called owing to their central position within the vertical succession of a cyclothem) are generally laterally extensive, in some cases being traceable from Oklahoma and Kansas northeastward to Iowa and Illinois (Heckel, 1977, 1994, 1995; Youle et al., 1994; Watney et al., 1995). The general environmental conditions associated with deposition of cyclothemic core shales have been examined in previous studies (., Heckel, 1977, 1991; Coveney et al., 1987; Hatch and Leventhal, 1992; Genger and Sethi, 1998; Cruse and Lyons, 2004). The detailed observations and inferences of the present study are drawn mainly from work on Missourian (lower Upper Pennsylvanian) core shales, especially the Hushpuckney, Stark, Muncie Creek and Eudora shales and their lateral equivalents (Algeo and Maynard, 1997, 2004; Hoffman et al., 1998; Algeo et al., 2004; Algeo, unpublished data) and, consequently, the sea in which these shales were deposited is referred to here as the "Late Pennsylvanian Mid-continent Sea" (LPMS).

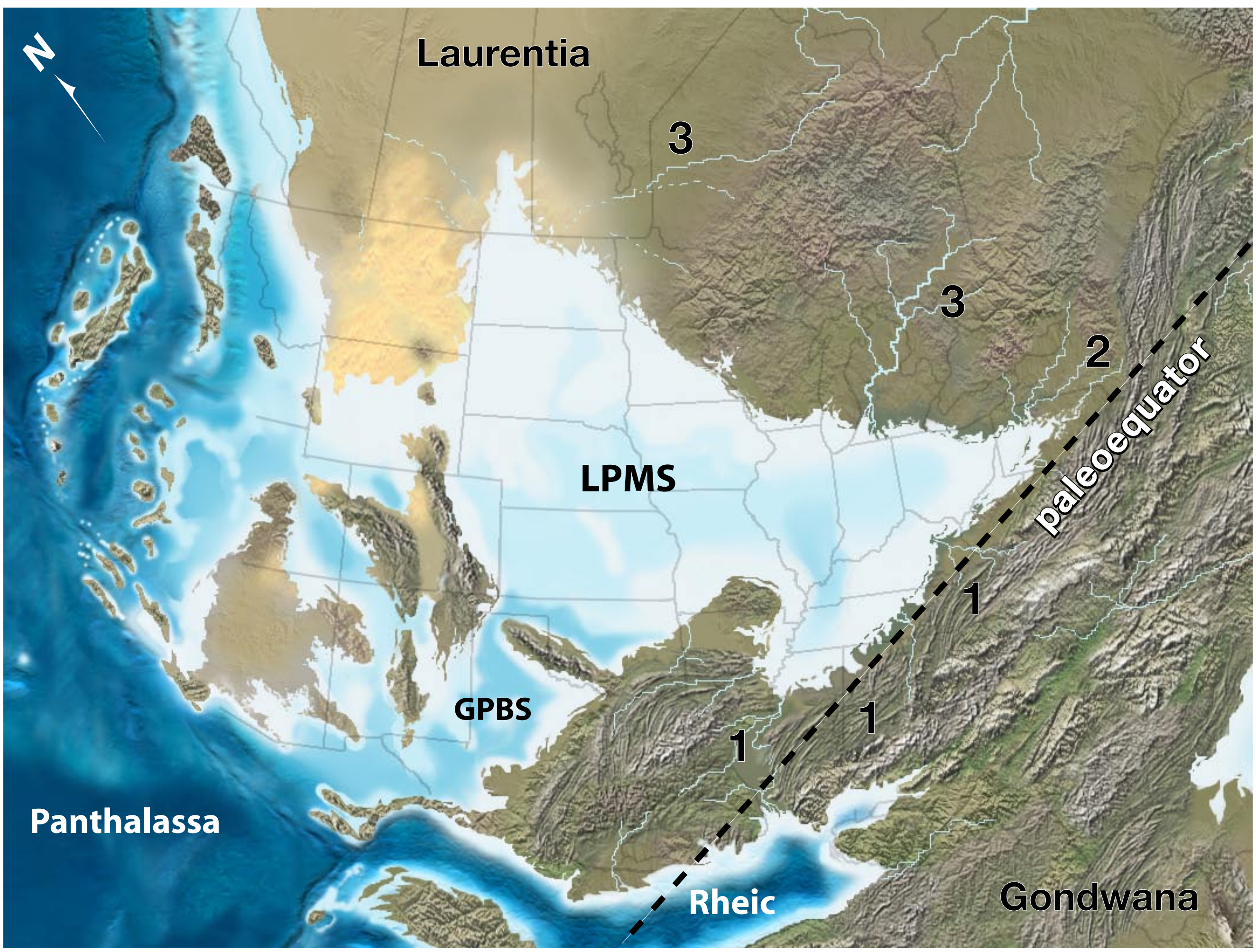

Figure 4. Regional paleogeography of North America during Late Pennsylvanian eustatic highstands. Major drainage systems: 1 = orogenic, 2 = foreland basin, and 3 = cratonic. Note connections to the global ocean through (1) an elongate, serpentine corridor in the Greater Permian Basin region, and (2) a broad, shallow and only intermittently open strait across the Wyoming Shelf. Names of features in and adjacent to the LPMS Shelf in Figure 5. N arrow represents paleonorth. This is a Lambert azimuthal equal-area projection modified from Blakey (2006). Major data sources: Cook and Bally (1975), Driese and Dott (1984), Ziegler (1988), Miller et al. (1992), Saleeby (1992), Scotese (1998), Dickinson and Lawton (2001), Heckel (2002) and Stampfli et al. (2002).

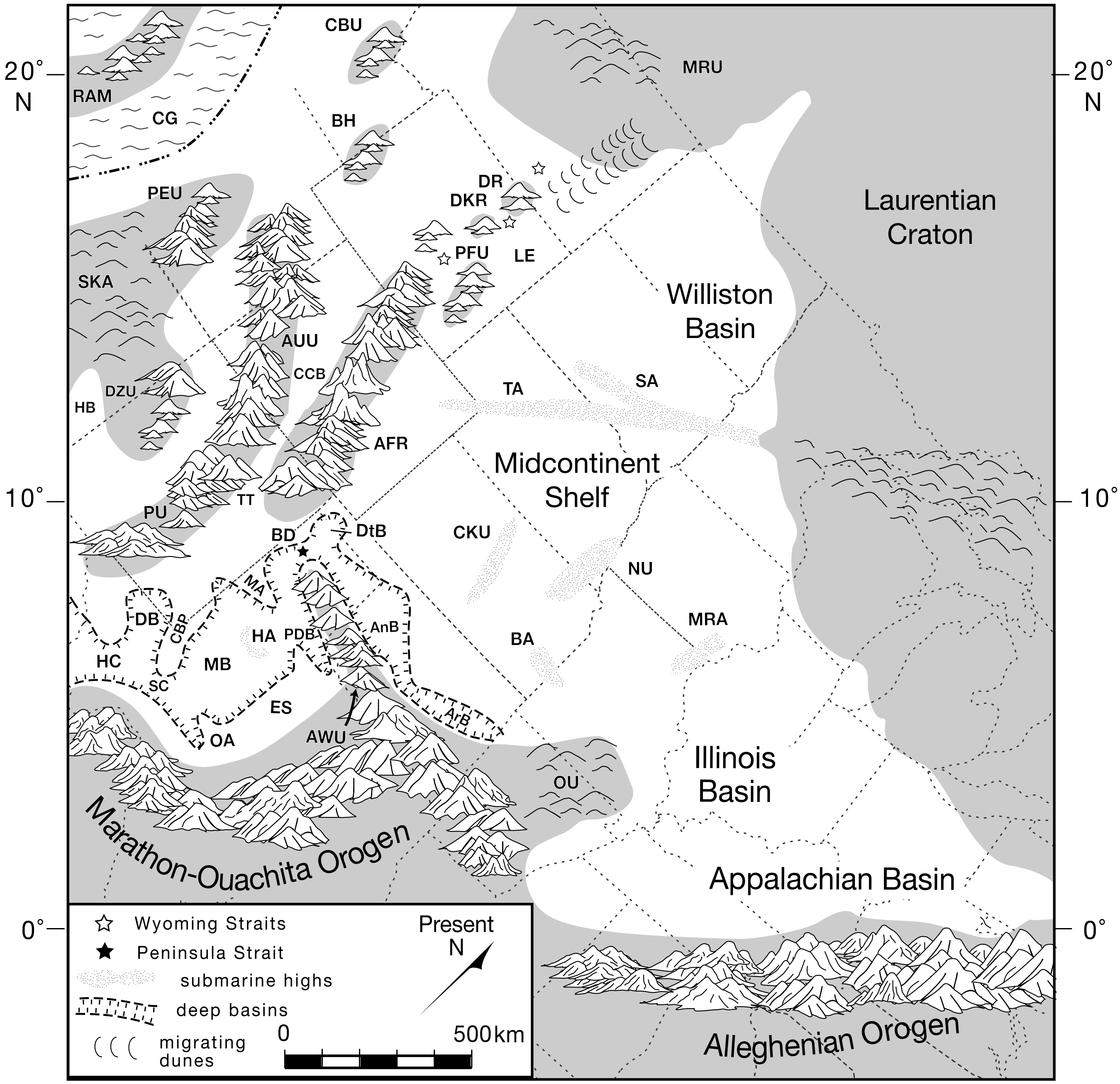

Figure 5. Paleogeography of the Late Pennsylvanian Mid-continent Sea of North America. Abbreviations for paleogeographic features: AnB = Anadarko Basin, ArB = Arkoma Basin, AFR = Ancestral Front Range, AUU = Ancestral Uncompahgre Uplift, AWU = Amarillo–Wichita Uplift, BA = Bourbon Arch, BD = Bravo Dome, BH = Bannock High, CBP = Central Basin Platform, CBU = Copper Basin Uplift, CCB = Central Colorado Basin, CG = Cordilleran Geosyncline, CKU = Central Kansas Uplift, DB = Delaware Basin, DtB = Dalhart Basin, DKR = Dull Knife Ridge, DR = Darton Ridge, DZU = Defiance–Zuni Uplift, ES = Eastern Shelf, HA = Horseshoe Atoll (or Scurry Reef), HB = Holbrook Basin, HC = Hovey Channel, LE = Lusk Embayment (or Alliance Basin), MA = Matador Arch, MB = Midland Basin, MRA = Mississippi River Arch, MRU = Milk River Uplift, NU = Nemaha Uplift, OA = Ozona Arch, OU = Ozark Uplift, PDB = Palo Duro Basin, PEU = Piute-Emery Uplift, PFU = Pathfinder Uplift, PU = Pedernal Uplift, RAM = Remnant Antler Mountains, SA = Siouxian Arch, SC = Sheffield Channel, SKA = Sedona-Kaibab Arches, TA = Transcontinental Arch, TT = Taos Trough. Major data sources: McKee et al. (1975), Heckel (1977, 1980), Casey (1980), Handford and Dutton (1980), Desmond et al. (1984), Maughan (1984, 1993), Garfield et al. (1988), Budnik (1989), Walker et al. (1995), Yang and Dorobek (1995), Hill (1999) and Blakey (2006).

GEOGRAPHIC, TECTONIC AND CLIMATIC BOUNDARY CONDITIONS

The LPMS had a maximum highstand area of ~2.1 x 10^6 km^2, making it more than twice as large as any of the modern epicontinental seas discussed above (Table 1). Most of the sea was underlain by shallowly flooded portions of the Laurentian craton, including areas comprising the Appalachian, Illinois and Williston basins as well as the mid-continent Shelf. The mid-continent Shelf itself consisted of a series of structural highs (e.g., the Nemaha and Central Kansas uplifts) and lows (e.g., the Forest City, Salina and Cherokee basins). All of these structural features were present during the Late Pennsylvanian, creating limited bathymetric relief across the LPMS seafloor. However, in areas of greater tectonic activity, such as the Appalachian Basin, deposition largely kept pace with crustal subsidence at this time (Faill, 1997; Greb et al., 2003). Only on the southwestern craton margin was subsidence sufficient to generate a series of deep-water basins, that is, the Dalhart, Anadarko and Arkoma basins, representing ~5% of the area of the LPMS. The low bathymetric relief of the cratonic portions of the LPMS allowed migration of the paleoshoreline over distances of hundreds of kilometres during Late Pennsylvanian glacio-eustatic transgressive–regressive cycles (Heckel, 1986; Boardman and Heckel, 1989; Joeckel, 1994, 1999; Watney et al., 1995).

The LPMS was nearly surrounded by landmasses, although these varied greatly in character (Figs. 4, 5). To the north and northeast, the Laurentian craton was emergent but of low relief. To the south and southeast, the Appalachian–Ouachita–Marathon orogens described a long, nearly continuous mountain arc (Arbenz, 1989). The Appalachian portion of this chain probably rose to high elevations, perhaps comparable to those of the modern Andes, whereas the Ouachita–Marathon section, which was part of a broad, not fully closed zone of convergence between Laurentia and the South American margin of Gondwana, was lower (Fig. 4; Speed et al., 1997). An outlier of this orogenic complex, the ~500 km long Amarillo–Wichita Uplift, was active during the Middle and Late Pennsylvanian and separated the LPMS from the Palo Duro, Midland, Delaware and Val Verde basins to the southwest (i.e., the Greater Permian Basin region; Handford et al., 1981; Budnik, 1989). To the northwest, the Ancestral Rocky Mountains and associated orogens (e.g., Sierra Grande, Pedernal Uplift) rose to moderate elevations during the Late Pennsylvanian. The Williston Basin, partially isolated by the submergent Siouxian Arch, formed the northern margin of the LPMS. Thus, the LPMS was largely isolated from the global ocean by surrounding landmasses (Figs. 4, 5).

The Pennsylvanian–Permian tectonics of western North America are complex (Burchfiel et al., 1992; Kluth, 1998). Two main phases of uplift and basin formation took place, an initial phase in the Desmoinesian (Middle Pennsylvanian) and a second phase during the Virgilian to Wolfcampian (Late Pennsylvanian to Early Permian) (Trexler et al., 1991; Yang and Dorobek, 1995). Uplift and basin development in the Ancestral Rocky Mountain region have been attributed to transpressional deformation associated with far-field effects of the Ouachita–Marathon orogeny to the south (Kluth and Coney, 1981; Kluth, 1986) and to convergent Andean-style deformation on the southwestern margin of North America (Ye et al., 1996, 1998). Reactivation of thrust faults in the Devonian–Mississippian Antler Orogen contributed to the formation of Late Pennsylvanian intra- and extra-orogenic flexural foredeeps in the Ancestral Rocky Mountains (Geslin, 1998; Hoy and Ridgway, 2002). Elsewhere in the southwest, there is evidence of concurrent transtensional deformation (Budnik, 1986; Stevenson and Baars, 1986; Algeo, 1992). The western continental margin, west of the Ancestral Rocky Mountains, was an obliquely convergent plate margin (Wallin et al., 2000).

The LPMS extended from the humid tropical zone at paleolatitudes of ~0–5°N to the dry tropical zone at paleolatitudes of ~15–20°N (i.e., Williston Basin area) (Fig. 5; Heckel, 1977, 1980). Along its southern margin, the peri-equatorial Appalachian–Ouachita–Marathon orogenic arc was within the paleo-intertropical convergence zone (Scotese, 1998). This resulted in a monsoonal climate, with moisture-laden air masses drawn from the proto-Tethyan embayment to the east over these orogens during the summer (Crowley et al., 1989, 1996; Parrish, 1993), resulting in high levels of precipitation and fluvial discharge into the LPMS. General atmospheric circulation climate models suggest that the mid-continent region had a tropical climate (10–25°C), limited seasonal temperature range (<15°C), and moderate annual precipitation (<73 cm y^{-1}) at this time (Crowley et al. 1989, 1996). A persistent subtropical high-pressure system resulted in dominance of trade winds from the northeast (Parrish and Peterson, 1988). Relative to the ever-wet conditions of the Middle Pennsylvanian, the Late Pennsylvanian climate of the mid-continent became drier and more seasonal as North America drifted northward out of the humid equatorial zone (Cecil, 1990; DiMichele and Phillips, 1996; Cecil et al., 2003b). However, climate conditions were generally humid during Missourian interglacial highstands (Cecil, 1990; Heckel, 1995; Soreghan et al., 2002; Algeo et al., 2004).

The closest modern analogue to the LPMS in terms of geographic, climatic and tectonic boundary conditions is the Gulf of Carpentaria (Fig. 1C; Edgar et al., 2003). Both seas spanned the same humid tropical to dry tropical climate zones, and both were bordered by elongate, active orogens. Despite such similarities, these seas exhibited very different bottom-water redox conditions: fully oxic in the modern Gulf of Carpentaria versus sulfidic in much of the LPMS.

Although the LPMS resembled the modern Baltic Sea with regard to benthic redox conditions, these seas contrast markedly with respect to their boundary conditions, the latter being located at mid- to high latitudes, in a cool-temperate to boreal climate zone, and distant from any active orogen (Fig. 1B). As the Baltic is the only large modern epicontinental sea to exhibit widespread seafloor anoxia, it appears that geographic, climatic and tectonic boundary conditions may be a less important influence on benthic redox conditions than other factors, such as regional hydrology, seafloor bathymetry, hydrography and primary productivity.

REGIONAL HYDROLOGY

The LPMS is likely to have received most of its freshwater discharge from: (1) a multitude of short, steep streams emanating from the periequatorial Ouachita and southern and central Appalachian orogens; (2) one or a few major foreland basin rivers with headwaters in the northern Appalachians; and (3) one or a few rivers draining large, mostly lowlying

Blakey, 2006). Discharge associated with streams emanating from the Ancestral Rocky Mountains, the Amarillo–Wichita Uplift, and other small emergent areas along the western margin of the LPMS was probably inconsequential for the hydrologic budget of the LPMS (e.g., Driese and Dott, 1984). However, rainfall directly over the LPMS itself may have made a significant contribution to this budget to the degree that this water was derived from extra-basinal sources and not through internal evaporation.

Tentative inferences about paleohydrologic fluxes are possible based on comparisons with modern river systems. The discharge of streams emanating from periequatorial areas of the Appalachian–Ouachita system can be estimated by comparison to humid tropical drainage systems in modern Sumatra, New Guinea or the equatorial Andes, which average ~200–300 cm of rainfall per year, or ~50–60 cm of run-off after accounting for evapo-transpiration (Ludwig and Probst, 1998; Cecil et al., 2003a). Based on an orogen length of ~2500 km (i.e., from the eastern Ouachitas in Oklahoma to the central Appalachians in New York; Figs. 4, 5) and a typical ridgeline-to-coastline distance of ~100–200 km (for modern active-margin orogens), the cumulative drainage area of these high-gradient streams was ~2.5–5.0 x 10^5 km^2 and their cumulative discharge into the LPMS was ~125–300 km^3 y^{-1}. Based on our paleogeographic reconstruction (Fig. 4), the drainage area of the major Appalachian foreland basin river(s) was ~1.0–1.2 x 10^6 km^2 (which is less than half the size of the Early Pennsylvanian foreland drainage system illustrated by Archer and Greb, 1995; *cf.* Gibling et al., 1992). Regression of discharge on drainage area for modern rivers (e.g., Milliman and Syvitski, 1992; Archer and Greb, 1995) suggests that a river system of this size would have had a discharge of ~200–800 km^3 y^{-1}, possibly toward the upper end of this range owing to the monsoonal climate of the watershed. A comparable, albeit slightly larger, modern river system is the Ganges–Brahmaputra, which has a drainage area of 1.7 x 10^6 km^2 and a discharge of 970 km^3 y^{-1} (Cecil et al., 2003a). Discharge estimates for cratonic rivers draining into the LPMS are more tenuous. Our paleogeographic reconstruction (Fig. 4) suggests one or two large cratonic watersheds with a cumulative area of perhaps 3–5 x 10^6 km^2, much of it within the dry tropical belt. A large modern river in a comparable climate zone is the Nile, which has a drainage area of 1.9 x 10^6 km^2 and a discharge of ~60 km^3 y^{-1}; scaling up yields an estimated discharge of ~100–150 km^3 y^{-1} for the Laurentian cratonic river(s). Finally, precipitation falling directly on the ~2.1 x 10^6 km^2 area of the LPMS may have averaged ~30–50 cm y^{-1} based on comparison with the modern Gulf of Carpentaria (Torgersen et al., 1988) and Carboniferous paleoclimate simulations (Crowley et al., 1989, 1996). If one-third of this rainfall was extra-basinally sourced, such as through monsoonal transport, then this represents an additional freshwater input of 100–170 km^3 y^{-1}.

Tallying these estimates of freshwater input into the LPMS yields an estimated annual flux of ~800–1500 km^3 (Table 1). Based on its estimated volume (105 x 10^3 km^3), it would take 70 to 130 years for fluvial discharge to fill the LPMS (i.e., the volume:discharge ratio), an interval comparable to that for the modern Gulf of Carpentaria (Table 1). It is possible that fluvial discharge into the LPMS was greater than estimated above owing to paleogeographic factors such as a >2500 km long orogen located within the paleo-intertropical convergence zone (Figs. 4, 5). An important point is that freshwater input was probably concentrated to some degree at the eastern (interior) end of the LPMS, a factor favouring formation of a reduced-salinity surface-water layer and mid-depth halocline across wide portions of this sea (Fig. 6) and conducive to strong spatial gradients in environmental conditions and sediment geochemistry (e.g., Algeo and Maynard, 1997; Hoffman et al., 1998; Cruse and Lyons, 2004). Independent evidence of strong freshwater discharge into the LPMS includes: (1) large concentrations of terrestrial organic matter (often 80–100% of TOC) in many cyclothemic core shales, reflecting export from coastal coal swamps (Algeo et al., 2004; cf. Greb et al., 2003); (2) strong lateral variation in benthic redox proxies and other sediment parametres, indicative of regional gradients in pycnocline strength and other watermass properties (Algeo and Maynard, 1997; Hoffman et al., 1998); and (3) uniformity of sediment ε_{Nd} values across the Appalachian and Ouachita basins, suggesting extensive reworking and transport of sediment westward across the mid-continent region (Dickinson et al., 2003).

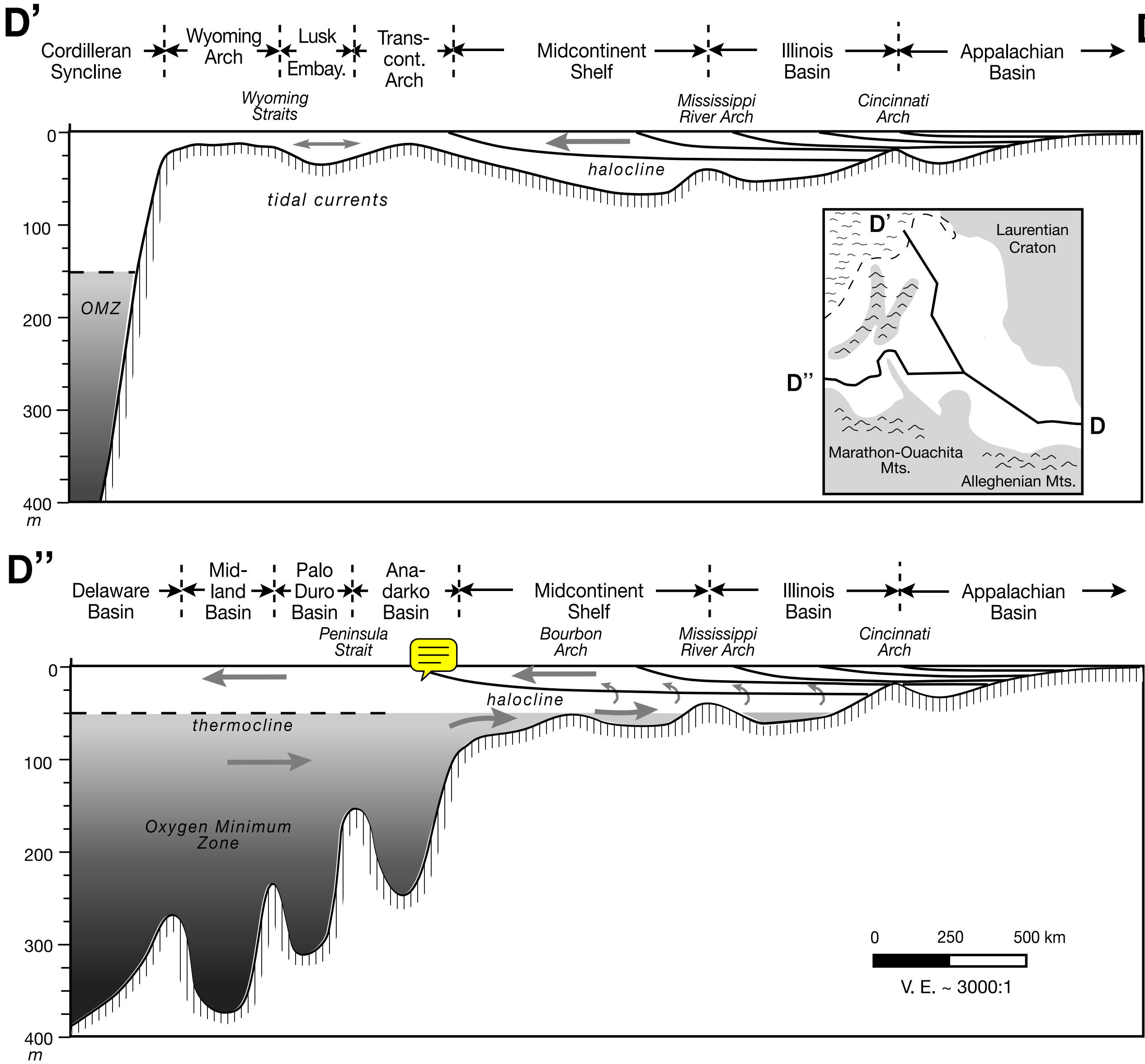

Figure 6. Schematic cross-sections of the Late Pennsylvanian Mid-continent Sea from the eastern interior region (D) through the two known passages to the global ocean, the 'Wyoming Straits' (new term; D') and the 'Panhandle Strait' (new term) and Hovey Channel (D"). Inferred watermass circulation patterns are shown by arrows. Seafloor bathymetry and watermass isopycnals are speculative but consistent with known geological observations and with inferences based on modern epicontinental sea analogues.

SEAFLOOR BATHYMETRY

The paleobathymetry of the LPMS seafloor, while locally variable, can be characterized in general terms. The thicker regressive portions of Upper Pennsylvanian cyclothems range from fossiliferous shales to carbonates, depending on the degree of climatic humidity (Feldman et al., 2005). Those that are carbonate commonly contain abundant phylloid algae with increasing numbers of dasycladacean green algae up-section, indicating water depths generally within the photic zone. A number of major cyclothems are capped by paleosols that are laterally extensive from northern Kansas to Nebraska and Iowa (Heckel, 1977, 1980; Schutter and Heckel, 1985; Joeckel, 1994, 1999). Although the water depths associated with core shale deposition are difficult to constrain narrowly based on facies character, it is likely that the Mid-continent Shelf was flooded to depths no greater than ~150 m during highstands based on observations of lowstand paleosol development and estimates of the amplitude of Late Pennsylvanian glacio-eustatic oscillations (Crowley and Baum, 1991; Soreghan and Giles, 1999; Joachimski et al., 2006). Stratigraphic evidence documents local areas of positive bathymetric relief, including the Central Kansas and Nemaha uplifts and the Bourbon and Mississippi River arches, indicating some regional variation in water depths. The average depth of the entire LPMS is tentatively estimated at ~50 m (Fig. 6), that is, similar to that of the modern Baltic Sea (55 m) or Gulf of Carpentaria (40 m) and shallower than that of Hudson Bay (120 m; Table 1). Water depths in the Arkoma and Anadarko foredeep basins to the southwest of the mid-continent Shelf margin may have been substantially greater, on the order of hundreds of metres, although this certainly varied through time in response to episodes of basin subsidence and fill (e.g., Arbenz, 1989).

Connections between the LPMS and the global ocean appear to have been quite limited. The Ancestral Rocky Mountains and associated uplifts formed a barrier extending from southern Wyoming to southern New Mexico, limiting watermass exchange to comparatively narrow areas to the north and south of these orogens (Figs. 4, 5). North of the orogens, the Tensleep/Minnelusa sequence was deposited on the Wyoming Shelf (or Arch) of central Wyoming and southern Montana during the Late Pennsylvanian (Mankiewicz and Steidtmann, 1979; Andrews and Higgins, 1984; Desmond et al., 1984; Maughan, 1993). It contains a mixture of eolian, arid-zone coastal and shallow-marine siliciclastic, carbonate and evaporitic facies that record at least a dozen marine transgressions across this area (Kerr and Dott, 1988). These sediments document the existence of a 200–300 km wide passage between the northwestern end of the LPMS in eastern Colorado and oceanic areas in Idaho and western Montana. Water depths through this passage were quite shallow, however, probably ~10 m or less during maximum eustatic highstands, and the passage was studded with shoals and islands (Figs. 4, 5; Desmond et al., 1984; Maughan, 1984, 1993; Garfield et al., 1988). These 'Wyoming Straits' (new term) were similar to the modern Torres Strait north of Australia. As ~70% of the Tensleep Sequence in central Wyoming represents eolian facies, this passage was subaerially exposed during much of the Late Pennsylvanian, and its existence was finally terminated by late Pennsylvanian-early Permian uplift of the Wyoming Arch (Blakey et al., 1988; Kerr and Dott, 1988).

A deep-water connection to the Williston Basin through central Montana (the Central Montana or Big Snowy Trough) was extant during the Early Pennsylvanian, but its existence during the Late Pennsylvanian is uncertain owing to later erosion of stratigraphic units of this age (Fanshawe, 1978; Peterson and MacCary, 1987; Luebking et al., 2001). The Williston Basin accumulated a thin succession of shallow-marine carbonates and evaporites and paralic sandstones at this time (Peterson and MacCary, 1987; Quandt, 1990), providing no evidence for the persistence of such a deep-water connection into the Late Pennsylvanian. The marked change in the character of Upper Pennsylvanian strata, from restricted-marine facies of the Williston Basin and the Lusk Embayment (or Alliance Basin; Fig. 5) in the north to the cyclothemic open-marine facies of the Mid-continent Shelf in the south, coincides with an area of stratigraphically thin deposits across western Nebraska and northeastern Colorado (Garfield et al., 1988). This suggests that the Transcontinental Arch was an east–west-trending paleobathymetric high at this time. The shoal-water character of Upper Pennsylvanian facies across the Arch is an indication of its extreme shallowness, which is likely to have contributed to diminished watermass exchange between the main body of the LPMS to the south and the more restricted Williston Basin–Lusk Embayment region to the north. Both the Williston Basin and the Wyoming Straits to its west were located at 15–20°N paleolatitude during the Late Pennsylvanian (Fig. 5).

A second, more important connection between the LPMS and the global ocean existed in the area south of the Ancestral Rocky Mountains (Figs. 4, 5). The gateway providing long-term, continual access to the LPMS was located between the western end of the Amarillo-Wichita Uplift and the eastern margin of the Bravo Dome. This 'Panhandle Strait' (new term) was a narrow (~30–40 km) but probably deep (>100 m) passage that existed continuously throughout the Late Pennsylvanian and into the Early Permian (Handford and Fredericks, 1980; Handford et al., 1981; Budnik, 1989). If water flow through the Wyoming Straits was strongly restricted (as inferred above), then the Panhandle Strait was likely to have been the chief regulator of watermass exchange between the LPMS and the global ocean. Before reaching the Panhandle Strait, however, waters moving cratonward traversed a serpentine, ~1000 km long corridor through the Greater Permian Basin region. This corridor commenced in the vicinity of the Hovey Channel, between the southern end of the Pedernal Uplift and the northwestern margin of the Ouachita–Marathon Front, at a paleolatitude of ~5–8°N, and then passed successively through the Midland, Palo Duro and Dalhart basins (Figs. 4, 5). Absolute water depths in this region are speculative for the most part (e.g., Fig. 6), but bathymetric variation is likely to have been considerable, with relatively deep basins (i.e., hundreds of metres) separated by shallower sills formed over structural highs (Handford and Dutton, 1980; Handford et al., 1981; Walker et al.

marine corridor through the Greater Permian Basin region is likely to have contained a continuous deep-water channel connecting the LPMS with the global ocean. The existence of such a channel is consistent with accelerated subsidence in this region during the Late Pennsylvanian and with a concomitant increase in local topographic relief (Algeo, 1992; Walker et al., 1995; Yang and Dorobek, 1995).

Shallow sills can strongly influence the hydrographic patterns and biotas of epicontinental seas. Although paleosill depths can be difficult to estimate, there is evidence against a shallow (i.e., <100 m deep) sill limiting watermass exchange between the LPMS and the global ocean. In modern epicontinental seas in which restricted exchange of the subpycnoclinal watermass results in hyposaline conditions (<~20‰ salinity; Drever, 1988), a low-diversity, euryhaline fauna is found, as in the modern Baltic (Hällfors et al., 1981). In modern estuaries, there is a slow loss of species diversity as salinity declines from 35‰ to 15‰ (Friedrich, 1965; Raffaelli, 1996). However, even then diversity is ~50% of the open-marine amount and marine organisms continue to dominate the biotic assemblage; the transition to a low-diversity community of brackish-water organisms generally occurs between 10‰ and 15‰ salinity. Salinity dynamics also play a role: watermasses with low but relatively stable salinities (typical of epicontinental seas) allow marine organisms to live closer to their lower tolerance limits than those with strong salinity fluctuations (typical of estuaries; e.g., Wallentinus, 1991). In the LPMS, faunal assemblages provide no evidence to support freshwater or brackish conditions during either eustatic highstands or lowstands. Although highstand anoxic core shales are characterized by an impoverished pelagic–nektic fauna consisting primarily of conodonts, ammonoids, fish debris and orbiculoid brachiopods, correlative limestones representing oxic facies contain a diverse normal-marine fauna of brachiopods, echinoderms, bryozoans, corals, molluscs, sponges and trilobites (Heckel and Baesemann, 1975; Heckel, 1977, 1980; Fahrer, 1996; Malinky and Heckel, 1998). Because this fauna is found as far east as the Appalachian Basin, it suggests that the highstand LPMS was not greatly reduced in salinity even in its interior (eastern) regions, an observation inconsistent with a silled perimeter and restricted watermass exchange. Furthermore, this same normal-marine fauna is associated with grey shales and carbonates deposited during regressive phases of the LPMS, when sea-level elevations had fallen by ~80–150 m relative to highstands (Crowley and Baum, 1991; Soreghan and Giles, 1999; Joachimski et al., 2006). Thus, the faunal evidence supports an open connection between the LPMS and the global ocean at all times during the Late Pennsylvanian.

A second argument against restricted exchange of the subpycnoclinal watermass in the LPMS is based on relationships between trace metal concentrations and benthic redox conditions. Trace metals such as Mo, U and V tend to become depleted in both the subpycnoclinal watermass and the sediment of strongly restricted silled basins, such as the modern Black Sea and Framvaren Fjord, through removal to the sediment without adequate resupply (Dyrssen et al., 1984). This process generally leads to a weakening of the relationship between sediment trace-metal concentrations and benthic redox status (Algeo and Lyons, 2006). One signature of this process in ancient sediments is a decline in trace-metal concentrations concurrent with intensification of benthic anoxia (as inferred from independent paleoredox proxies such as degree-of-pyritization) (Algeo, 2004). In Upper Pennsylvanian core shales of the mid-continent region, however, the concentrations of all redox-sensitive trace metals are tightly coupled to benthic redox conditions (Algeo et al., 2004), implying sufficient watermass exchange as to prevent depletion of dissolved trace metals in subpycnoclinal waters of the LPMS during highstands. If deep-water renewal was also unimpaired during lowstands (as suggested by faunal evidence discussed above), then sill depths must have been greater than ~100 m, possibly much so, during highstands (Table 1). Because the only likely location of a deep-water channel to the global ocean is through the Panhandle Strait and Greater Permian Basin region, we infer minimum highstand water depths of ~100 m or more along the length of this corridor (Fig. 6).

HYDROGRAPHY

Aspects of the hydrography of the LPMS can be reconstructed with a fair degree of assurance. The existence of a strong pycnocline during highstands is supported by several arguments. First, laminated black core shales representing the deepest water facies of mid-continent cyclothems exhibit sharp lower and upper contacts, suggesting a rapid change between oxic–suboxic and anoxic conditions on the LPMS seafloor (Heckel, 1977; Algeo et al., 2004; Cruse and Lyons, 2004). The most likely explanation is that the pycnocline, which separated an oxygenated surface-water layer from oxygen-depleted deeper waters, migrated first toward and then away from the craton during each eustatic transgressive–regressive cycle, leaving its signature in the sediment as an abrupt change in redox conditions wherever it intersected the Mid-continent Shelf. Second, centimetre-thick compositional cycles in these shales are correlatable over distances of at least a few hundred kilometres (e.g., Algeo and Maynard, 1997, p. 135–136), a degree of bedding continuity known only from the modern Black Sea (Lyons, 1991, fig. 4). Lateral continuity of fine sediment layers at this scale implies uniformity of environmental conditions and synchroneity of changes in watermass properties over wide areas, a pattern that is likely to develop only beneath a persistently stable, strong pycnocline. Third, sulfidic conditions existed in subpycnoclinal waters of the LPMS during deposition of laminated black core shales, as shown by exceptionally high levels of trace-element enrichment and the presence of syngenetic pyrite (Algeo and Maynard, 2004; Algeo et al., 2004). These conditions existed despite low levels of primary productivity and benthic oxygen demand in the LPMS (see below). In order to maintain such oxygen-deficient conditions over wide areas for long intervals, vertical mixing must have been significantly reduced and, hence, the LPMS pycnocline must have been relatively strong. Stratification of the LPMS was probably due to major fluvial discharge into this nearly landlocked sea, and by unrestricted influx of colder intermediate-depth waters of marine salinity below a thermocline, producing a large-scale estuarine-type circulation pattern (Fig. 6).

Earlier workers have proposed that water-column stratification was maintained in interior (eastern) areas of the LPMS by a halocline and in exterior (western) areas by a thermocline (Heckel, 1991; Heckel and Hatch, 1992; Hatch and Leventhal, 1992; Hoffman et al., 1998). However, the modern Baltic Sea demonstrates that, given a strongly positive water balance, a halocline can be supported across wide areas. Further, great water depths are not necessary for development of a permanent halocline in an epicontinental sea. Haloclines are present in the modern Hudson Bay and Baltic Sea at depths of ~15–30 m and ~40–80 m, respectively, so highstand water depths ~80–150 m on the outer Mid-continent Shelf of the LPMS would have been sufficient for development of a permanent halocline at ~15–50 m (Table 1). Given that freshwater discharge into the LPMS was concentrated somewhat at its interior (eastern) end (see above), the depth of the halocline must have shallowed westward toward its connection with the global ocean (Fig. 6; *cf.* Figs. 2A, B). One additional factor that is likely to have contributed to maintenance of a permanent halocline in the open LPMS was microtidality, which limits tidal mixing of the water column and is characteristic of largely landlocked water bodies such as the LPMS (Kennett, 1982; Wells et al., 2005a,b and herein; Table 1).

Quantitative estimates of pycnocline strength in the LPMS and of the watermass properties controlling it are necessarily tentative. Modern estuaries can have exceptionally strong pycnoclines, with deep-to-shallow density differentials ($\Delta\sigma_t$) of more than 20 units, as a consequence of a fresh surface-water layer overlying a deep-water layer of near-marine salinity (Kennish, 2001; recalling that σ_t is calculated as watermass density in units of kg m^{-3} minus 1000). Larger water bodies exhibit smaller $\Delta\sigma_t$ owing to lower (volume-normalized) freshwater influx and greater (area-normalized) vertical mixing: the modern Baltic Sea and Hudson Bay have $\Delta\sigma_t$ of ~4 units (Table 1), of which ~80% and 20% are attributable to vertical gradients in salinity and temperature, respectively (*n.b.*, all watermass densities calculated from the international equation of state of seawater, UNESCO, 1981, as given in Chester, 1990). This $\Delta\sigma_t$ value may represent a minimum estimate for the LPMS, which must have been strongly stratified to achieve widespread sulfidic conditions in its bottom-water despite low benthic oxygen demand (discussed below). A significant constraint on salinity and σ_t estimates for the LPMS is the presence of a diverse normal-marine biota in highstand limestones of the Appalachian Basin, suggesting that surface-waters in interior areas of the sea were probably not greatly reduced (probably ≤10‰) in salt content relative to contemporaneous seawater. Several lines of evidence suggest that seawater salinities were higher in the past than the present value of ~35‰ (Knauth, 1998; Hay et al., 2001, 2006). According to the models of Hay et al. (2001, 2006), Late Pennsylvanian seawater had a salinity of ~45–50‰. Based on these considerations, estimated watermass properties of the LPMS are 35–40‰ S, 25°C, and 23–27 σ_t for surface-waters and 45–50‰ S, 15°C and 34–38 σ_t for deep-waters, yielding a deep-to-shallow density differential ($\Delta\sigma_t$) of ~11 ± 4 units (Table 1), of which ~70% and 30% are attributable to vertical gradients in salinity and temperature, respectively.

Circulation patterns in the LPMS can be inferred based on hydrologic and climatic factors and on regional variation in sediment properties. Hydrologic considerations suggest that freshwater discharge into the LPMS was concentrated to some extent at its interior (eastern) end resulting in a westward net flow of surface-waters (Heckel, 1977, 1980). In addition to net transport, most inland seas also exhibit gyral circulation, such as cyclonic (counter-clockwise in the Northern Hemisphere) as in Hudson Bay and the Baltic Sea, anticyclonic, or seasonally reversing as in the Gulf of Carpentaria (Alhonen, 1966; Church and Forbes, 1981; Prinsenberg, 1986). In the LPMS, spatial variation in sediment geochemistry favours a cyclonic circulation pattern (cf. Heckel, 1980, fig. 5). Redox proxies (e.g., degree-of-pyritization, trace-metal concentrations) indicate that benthic anoxia intensified to the north, suggesting a stronger pycnocline in that direction (Algeo and Maynard, 1997; Hoffman et al., 1998; Cruse and Lyons, 2004). Further, both illite and vitrinite increase to the north (relative to smectite and inertinite, respectively), suggesting a larger contribution of coarser, water-borne clays and organic debris relative to a finer, possibly wind-blown fraction (Algeo and Maynard, 1997). A cyclonic flow pattern implies an important influence of the easterly trade winds, perhaps modified to some degree by seasonal monsoonal circulation. Another factor contributing to cyclonic flow may have been the Coriolis Effect, which is operative as close to the equator as ~8°N (W.W. Hay, pers. comm., 2005) and would have pushed river waters entering the LPMS from the north in a westward direction, along the northern margin of the LPMS.

Deep-water flux is a hydrographic parameter that is difficult to quantify even in modern marine environments. Because inland seas generally have well-defined hydrologic sources and sinks, a simple mass-balance model based on salinity differences between the surface and deep-water layers can be used to estimate the deep-water flux (cf. Ehlin, 1981). The essential equations are:

$$Q_s \qquad {}_f + Q_d \text{ (volume mass balance)} \qquad (1)$$

$$Q_s \bullet S_s = Q_f \bullet S_s + Q_d \bullet S_d \text{ (salinity mass balance)} \qquad (2)$$

where Q is water flux, S is salinity and the subscripts *f*, *s* and *d* indicate freshwater inflow, surface-water outflow and deep-water inflow, respectively. In modern marine systems, all parametres other than Q_d may be known. For the LPMS, none of these parametres is known with assurance (except that freshwater salinity, S_f, was close to 0‰), but estimates for Q_f (~800–1500 km^3 y^{-1}), S_s (~35–40‰) and S_d (45–50‰) were derived in the discussion above (Table 1). Given these input values, the two remaining variables (Q_s and Q_d) can be solved for. This calculation yields estimates for Q_d and Q_s of ~0.09–0.19 and ~0.11–0.24 x 10^6 m^3 s^{-1}, with median values of 0.14 and 0.17 x 10^6 m^3 s^{-1}, respectively. Although tentative, these estimates suggest that the deep-water flux into the LPMS was comparable to that for modern Hudson Bay and the Baltic Sea (Table 1). If the 30–40 km wide Panhandle Strait was the chief regulator of watermass exchange between the LPMS and the global ocean (see above) and its depth was 200 m, then flow rates in each direction through this strait would have been on the order of 0.02–0.07 m s^{-1}. These rates are comparable to rates observed in modern deep-water channels such as Hudson Strait (Collin, 1966; Drinkwater, 1986).

Transit of deep-ocean waters through a ~1000 km long corridor in the Greater Permian Basin region prior to advection onto the southern margin of the Mid-continent Shelf may have altered the physicochemical characteristics of the watermass reaching the LPMS. For this reason, consideration of hydrographic conditions in the Late Pennsylvanian Greater Permian Basin Seaway is necessary. Some type of water-column stratification appears to have existed in the deeper basins of this area, all of which are characterized by thin Upper Pennsylvanian successions of organic-rich shales and siltstones reflecting benthic oxygen depletion and sediment starvation (Adams et al., 1951; Jackson, 1964; Cys and Gibson, 1988; Landis et al., 1992; Hamlin et al., 1995; n.b., it appears that sandstones and carbonate debris flows and turbidites of these basins are associated with active basin-margin uplifts; Winfree, 1998). A thermocline controlled by lateral advection of intermediate-depth waters from the eastern Panthalassic Ocean is likely to have existed (Fig. 6; Heckel, 1980), although a halocline may have been present too, given that the Greater Permian Basin was located within the paleo-intertropical convergence zone and largely rimmed by orogenic highlands at that time (Figs. 4, 5). Significantly, the shallow marginal shelves of some basins, for example, the Eastern Shelf of the Midland Basin, accumulated thin phosphatic black shales similar to mid-continent cyclothemic core shales during glacio-eustatic highstands (Jackson, 1964; Boardman and Heckel, 1989), which might be construed as evidence of a shallow halocline for the same reasons that pertain to the Mid-continent Shelf (see above). The significance of water-column stratification in the Greater Permian Basin Seaway is that subpycnoclinal waters traversing the ~1000 km long corridor between the open ocean and the LPMS are likely to have become progressively more oxygen-depleted as a result of benthic oxygen demand, resulting in a preconditioning of the watermass that may have played an important role in the redox dynamics of the LPMS (see below). However, inferences regarding hydrographic conditions in the Greater Permian Basin Seaway must remain tentative pending more detailed study of that region.

PRIMARY PRODUCTIVITY

A significant influence on seafloor redox conditions is benthic respiratory oxygen demand, the latter largely a function of primary productivity rates and C_{org} sinking fluxes. Although there is no proxy that can provide a reliable estimate of primary productivity in paleoseas, C_{org} sinking fluxes can be estimated on the basis of C_{org} burial fluxes and inferred preservation efficiencies (Canfield, 1994; Hay, 1995). C_{org} burial fluxes are calculated from average TOC values and estimated sedimentation rates. TOC values in Missourian Stage cyclothemic core shales are mostly in the range of 5–30 wt%, with a few samples containing as much as 40 wt% TOC (Table 1). However, much of this organic matter is of terrestrial origin and, hence, unrelated to marine productivity; the proportion of marine algal matter in any given sample is highly variable but averages about 30–40% of TOC for Missourian core shales as a whole (Algeo, unpublished data).

There is ample evidence that sedimentation rates were exceptionally low during deposition of cyclothemic core shales, such as: (1) an abundance of authigenic phosphate, with some core shales containing >50 phosphatic granule layers (Heckel, 1977, 1991; Kidder, 1985; Kidder et al., 1996; Algeo et al., 2004), each possibly requiring hundreds to thousands of years to form (cf. Föllmi, 1996; Filippelli, 1997); (2) large concentrations of higher land plant debris (i.e., vitrinite and inertinite), which must have been rafted or blown into the LPMS (Algeo and Maynard, 1997; Hoffman et al., 1998; Algeo et al., 2004); and (3) enrichment of redox-sensitive trace metals (e.g., Mo, U, V and Zn) to a degree rarely encountered outside of hydrothermal ores (Coveney et al., 1987; Hatch and Leventhal, 1992; Genger and Sethi, 1998; Algeo and Maynard, 2004; Algeo et al., 2004; Cruse and Lyons, 2004). These features point to a sediment-starved, distal offshore environment in which terrestrial organic matter and hydrogenously sourced trace metals became highly concentrated owing to an exceptionally low influx of siliciclastic material. Sedimentation rates can be estimated tentatively on the basis of cyclostratigraphic analysis (Algeo et al., 2004; Heckel, 2004). If small-scale compositional cycles reflect short-period orbital forcing, for example the ~20-ky precession cycle, then the present (., compacted) sedimentation rate of core shales is ~0.002–0.008 mm y^{-1}. This is slightly lower than the Holocene sedimentation rate on the Black Sea abyssal plain, which is ~0.1 mm y^{-1} at present porosities of ~90%, equivalent to ~0.01 mm y^{-1} on a fully dewatered basis (Shimkus and Trimonis, 1974; Karl and Knauer, 1991; Arthur et al., 1994).

Combining a sedimentation rate estimate of ~0.002–0.008 mm y^{-1} with a measured bulk density of 2200 kg m^{-3} and average TOC values of 5–30% yields calculated C_{org} burial fluxes for LPMS core shales in the range of 0.2–5.3 g C m^{-2} y^{-1} (median: 1.1 g C m^{-2} y^{-1}), of which only 30–40% or 0.06-2.1 g C m^{-2} y^{-1} (median: 0.4 g C m^{-2} y^{-1}) represents the marine C_{org} flux (Table 1). Independent evidence of low C_{org} fluxes to the sediment is provided by authigenic sulfides (i.e., pyrite), which are strongly ^{34}S-depleted relative to Late Pennsylvanian seawater sulfate ($\Delta^{34}S = 40 \pm 5$ ‰; Coveney and Shaffer, 1988; Coveney et al., 1991). Strongly ^{34}S-depleted pyrite is indicative of low bacterial sulfate reduction rates, suggesting a low flux of labile, easily degradable marine organic matter to the sediment (Anderson and Pratt, 1995). Because preservation efficiencies are relatively high (~10-30%) in sulfidic environments, even at low sedimentation rates (Canfield, 1994), the C_{org} burial fluxes calculated above imply C_{org} sinking fluxes of <21 g C m^{-2} y^{-1} with a median estimate of ~1 g C m^{-2} y^{-1} (Table 1). Primary productivity per se cannot be estimated, but, in view of the strongly euxinic bottom-water conditions and shallow pycnocline of the LPMS, the fraction of primary productivity represented by the C_{org} sinking flux is likely to have been higher than in most modern seas; hence, primary productivity rates in the LPMS are likely to have been quite low.

Upwelling can be an important factor in the formation of organic-rich deposits on modern continental margins (Hay, 1995). Earlier studies of the LPMS proposed upwelling of nutrient-rich deep-waters from adjacent basins onto the southern margin of the Mid-continent Shelf (Heckel, 1977, 1991). However, various climatic and sedimentologic considerations support a mechanism and intensity for this process that was quite different from upwelling on the modern Peru or Namibian shelves. First, continental-margin upwelling systems are the product of offshore, wind-driven Ekman transport of surface-waters on arid tropical shelves. Climatic aridity is a key factor as strong fluvial discharge would produce a density-stratified inner-shelf watermass that would suppress upwelling. Deep-water flow in the LPMS was unrelated to Ekman transport. Rather, it was a result of entrainment of the subpycnoclinal watermass by large-scale estuarine-type circulation in a largely landlocked epicontinental sea (Fig. 6). Second, continental-margin upwelling systems are characterized by a patchy, eddy-controlled distribution of upwelling and downwelling cells (Summerhayes et al., 1995), resulting in laterally discontinuous deposits of organic-rich sediment (Bailey, 1991; Smith, 1992; Glenn et al., 1994). This is a pattern unlike the widely correlatable centimetre-thick layers of Upper Pennsylvanian core shales (Algeo and Maynard, 1997, p. 135–136), although a certain patchiness of black and grey facies exists in some core shales along the southern margin of the Mid-continent Shelf in the Kansas–Oklahoma border region (Heckel, unpublished data). Third, estimates of primary productivity and C_{org} burial fluxes for the LPMS are exceptionally low (see above), far lower than in modern upwelling systems (e.g., Calvert and Price, 1983; Marlow et al., 2000), implying a low flux of nutrient-rich waters onto the Mid-continent Shelf margin. These considerations suggest that upwelling of deep-waters was of limited importance in the LPMS, and that lateral advection of preconditioned, oxygen-deficient intermediate waters was a more important influence on benthic redox conditions (see below).

COMPARISON OF MODERN AND ANCIENT EPICONTINENTAL SEAS

HOW WAS THE LATE PENNSYLVANIAN MID-CONTINENT SEA DIFFERENT?

None of the three large modern epicontinental seas examined in this study (i.e., Hudson Bay, the Baltic Sea and the Gulf of Carpentaria) appear to be a good analogue for the full suite of environmental conditions and dynamics of the LPMS. Although the Gulf of Carpentaria exhibits similar geographic, climatic and tectonic boundary conditions (Edgar et al., 2003), differences in hydrology and hydrography result in a weakly stratified water column and a well-oxygenated seafloor. The Hudson Bay and Baltic Sea are dissimilar to the LPMS in terms of their boundary conditions, being located at mid- to high latitudes, in temperate to boreal climate zones, and distant from any active orogen. As the Baltic is the only large modern epicontinental sea subject to seafloor anoxia, it appears that geographic, climatic and tectonic

benthic redox conditions of such marine systems compared to hydrologic, bathymetric, hydrographic and productivity factors.

Regional hydrology, especially the volume of freshwater discharge, is an important influence on watermass stratification in epicontinental seas. Estimated discharge into the LPMS was 800–1500 km^3 y^{-1}, that is, greater than that for large modern epicontinental seas with the possible exception of Hudson Bay. Significant discharge into the LPMS was favoured by a monsoonal climate, the location of the >2500 km long Ouachita–Appalachian orogen within the paleo-intertropical convergence zone, and, perhaps, intensified evapo-transpiration associated with widespread coastal coal swamps during Late Pennsylvanian glacio-eustatic highstands (Cecil, 1990; Cecil et al., 2003b; Archer and Greb, 1995; DiMichele and Phillips, 1996; Soreghan et al., 2002; Algeo et al., 2004). Relative to its size, however, the LPMS does not appear to have received exceptionally large amounts of freshwater runoff. Its basin volume-to-discharge ratio (~70–130 y) is similar to that for Hudson Bay and the Gulf of Carpentaria and exceeds that for the Baltic Sea. Additional factors that may have helped to sustain a halocline over wide areas of the LPMS include a largely landlocked setting, concentration of river discharge at its interior (eastern) end and weak tidal mixing.

Tidal currents can be a potent force in maintaining a well-mixed watermass (Wells et al., 2005a,b, herein). This is evident in the Gulf of Carpentaria, where strong tidal currents through Torres Strait inhibit formation of an extended halocline in the northern gulf despite elevated river discharge from the New Guinea highlands (Somers and Long, 1994; Porter-Smith et al., 2004). In Hudson Bay, a mesotidal range on the western basin margin contributes to high benthic dissolved oxygen levels and accumulation of coarse, TOC-lean sediments (Pelletier et al., 1968; Anderson and Roff, 1980; Pelletier, 1986; Prinsenberg, 1986; Roff and Legendre, 1986; Biksham and d'Anglejan, 1989). More completely landlocked seas such as the Baltic are subject to reduced tidal influence. Although the LPMS may have had a deep-water connection to the global ocean, the tortuous path of this corridor through the Greater Permian Basin region is likely to have prevented much penetration of open-ocean tides into its interior. Thus, the paleogeographic geometry of the gateway to the LPMS and its influence on tidal ranges may have influenced vertical mixing and pycnocline strength.

Pycnocline strength can be an important influence on benthic redox conditions, as a large vertical density contrast can severely restrict vertical mixing and, hence, the downward flux of dissolved oxygen. Vertical density contrast is closely related to the mechanism of water-column stratification, and marine systems with haloclines tend to exhibit more stable and durable stratification than those with shallow thermoclines that typically develop and degrade seasonally. The relatively large deep-to-shallow density differentials ($\Delta\sigma_t$) of Hudson Bay (~4.5 units) and the Baltic Sea (~4.0 units) reflect the existence of permanent haloclines in these water bodies, whereas the smaller density differential of the Gulf of Carpentaria (~1.5 units) reflects development only of a shallow, seasonal thermocline. Inferred watermass properties for the LPMS yield σ_t values of ~23–27 and 34–38 for the shallow and deep layers, respectively, implying a $\Delta\sigma_t$ on the order of 11 ± 4 units, that is, a density differential significantly greater that than for any modern epicontinental sea. Thus, a strong pycnocline and reduced vertical mixing were important factors contributing to development of widespread benthic anoxia in the LPMS.

Seafloor bathymetry influences deep-water renewal through the presence or absence of marginal sills. In the Baltic Sea, shallow (<30 m) sills regulate watermass exchange with the Kattegat–Skagerrak–North Sea (Fig. 2B). Deep-water renewal occurs as discrete events, when regional meteorological conditions allow denser North Sea waters to spill through the Danish Straits, at intervals of a few years to decades. Following discrete recharge events, the deep-watermasses of basins of the Baltic Proper become suboxic for intervals of a few months to years before returning to an anoxic condition. Without marginal sills, Baltic Sea deep-waters almost certainly would not be anoxic at present. Marginal sills are of little consequence in the Gulf of Carpentaria, where sill depth is great (53 m) relative

deep marginal sills (>200) allow substantial deep-water renewal (Figs. 2A, 2C). In the LPMS, the northwestern passage (Wyoming Straits) connecting it to the global ocean was probably no deeper than ~10 m or so at highstands, thus forming a shallow marginal sill that restricted exchange of subpycnoclinal waters. However, the corridor connecting the LPMS to the global ocean through the Greater Permian Basin region was probably much deeper (>100 m) along its ~1000 km length, with watermass exchange regulated by the narrow but deep strait at the western end of the Amarillo–Wichita Uplift. Thus, shallow marginal sills and restricted deep-water exchange probably were not important factors in the development of widespread benthic anoxia in the LPMS.

One factor related to seafloor bathymetry, the thickness of the subpycnoclinal water column, may have influenced benthic redox conditions in the LPMS. The depth of the pycnocline relative to average water depth determines the volumetric proportions of the oxygenated surface-water layer and the potentially oxygen-depleted deeper watermass of a stratified water body. When the fractional volume of the subpycnoclinal layer is large, the deeper watermass is buffered to a greater degree against respiratory oxygen demand; conversely, when its fractional volume is small, the deeper watermass is more prone to depletion of dissolved oxygen. These relationships are well illustrated by modern epicontinental seas. In Hudson Bay, for example, pycnocline depth (15–30 m) is shallow compared to average water depth (120 m), resulting in the deep-water layer comprising >80% of basin volume (Table 1). In contrast, the Baltic Sea has a deeper pycnocline (40–80 m) and lesser average water depth (55 m), resulting in the subpycnoclinal watermass comprising only ~25% of basin volume. These relationships make Baltic Sea deep-waters fundamentally more prone to anoxia as a consequence of respiratory oxygen demand. Although estimates for the LPMS are tentative, a pycnocline depth of ~15–30 m on an evenly inclined ramp with a 100 m deep outer margin implies that the subpycnoclinal watermass comprised ~50–75% of total basin volume, an estimate between those for Hudson Bay and the Baltic Sea. However, on an inclined ramp the thickness of the subpycnoclinal water column relative to the overlying surface-water layer would have diminished in the cratonward direction (e.g., Fig. 6), so that the fractional volume of the subpycnoclinal watermass in interior portions of the LPMS may have been much smaller. This may have facilitated deep-water oxygen depletion in the LPMS despite low levels of primary productivity.

Primary productivity is an important control on benthic oxygen demand and, hence, deep-water redox conditions. Modern epicontinental seas exhibit considerable variation

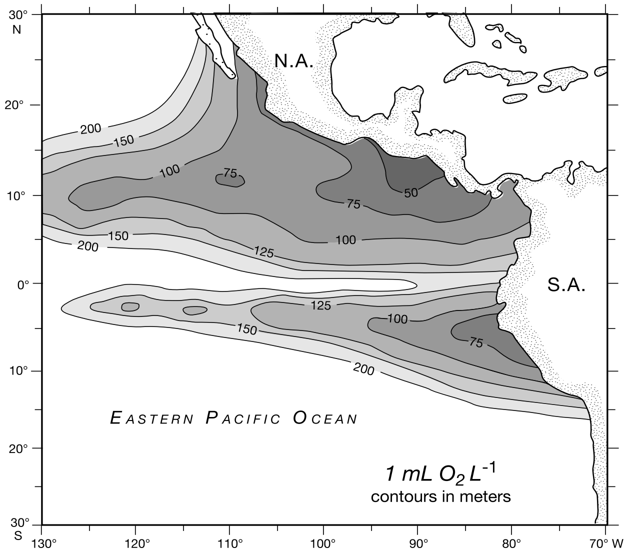

Figure 7. Depth to the top of oxygen minimum zone (OMZ) in the modern eastern equatorial Pacific Ocean, as defined by the 1 mL L^{-1} dissolved oxygen isocon; contours in metres. There is extreme shallowing of the OMZ at latitudes of ~3–12°S and 5–22°N. The contoured surface is co-extant with a strong thermocline. Data from Levitus and Boyer (1994).

in primary productivity rates that may account, in part, for differences in their benthic redox status. The highest productivity levels are found in the Gulf of Carpentaria (200–670 g C m^{-2} y^{-1}), but benthic oxygen demand is more than compensated for by vertical mixing across a weak pycnocline and by strong lateral advection of oxygenated deep-waters. Although productivity levels are somewhat lower in the Baltic Sea (120–240 g C m^{-2} y^{-1}), its C_{org} burial flux is the largest among modern epicontinental seas (~12–32 g C m^{-2} y^{-1}) owing to the higher preservation efficiencies associated with anoxic facies (Canfield, 1994). Thus, high levels of primary productivity alone are inadequate to establish benthic anoxia in modern epicontinental seas, and strong restriction of the deep-watermass appears to be a necessary condition. Given the apparent lack of both high productivity levels and watermass restriction in the LPMS (see above), it seems clear that benthic anoxia in epicontinental seas cannot be attributed to a single factor or set of factors, and that various, widely differing environmental scenarios may permit its development.

Given that some of the factors most commonly contributing to marine benthic anoxia (e.g., high productivity, severe watermass restriction) appear not to have been important in the LPMS, it is useful to consider whether other, less common by cited factors were operative. One may have been the oxygen-deficient character of the deeper watermass that was laterally advected into the LPMS. This ‘preconditioned’ oxygen deficiency was due to two causes. First, the oxygen

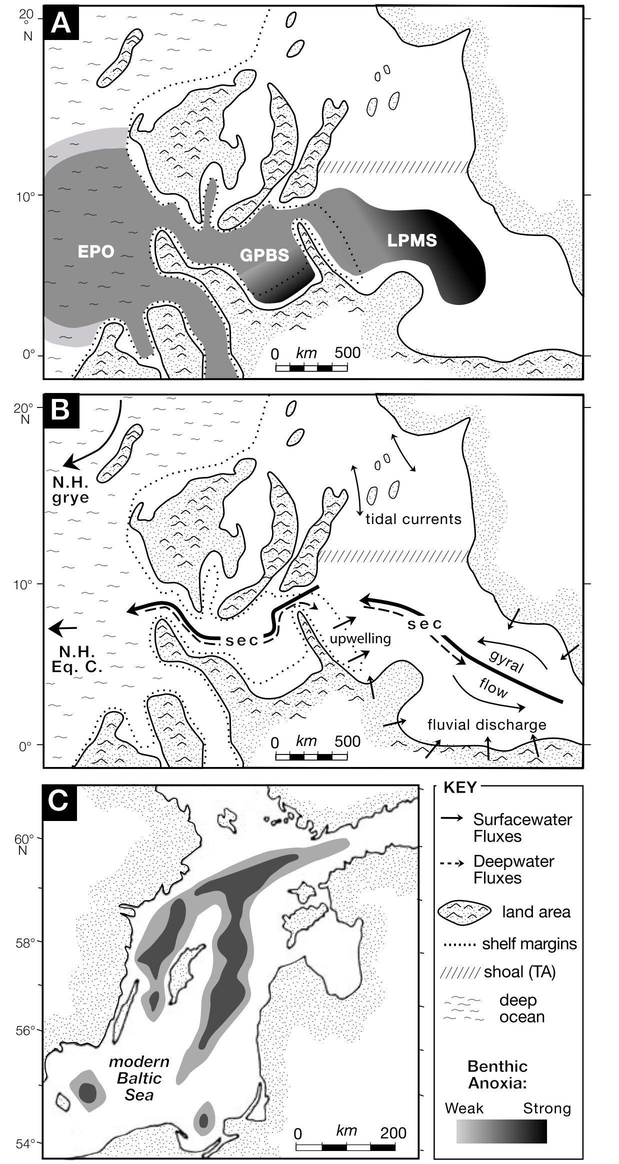

Figure 8. Benthic redox variation (A) and watermass circulation patterns (B) in western Laurentia during the Late Pennsylvanian. EPO = Eastern Panthalassic Ocean, GPBS = Greater Permian Basin Seaway, LPMS = Late Pennsylvanian Mid-continent Sea, N.H. Eq. C. = Northern Hemisphere Equatorial Current, sec = super-estuarine circulation, and TA = Transcontinental Arch. Redox patterns in the LPMS and GPBS are approximately known from geological data; redox patterns in the EPO and elsewhere are speculative. The LPMS exhibits a strong lateral redox gradient with the most intense anoxia in shallow interior-shelf regions to the east. (C) Benthic redox variation in the modern Baltic Sea. In contrast to the LPMS, the Baltic exhibits a basin-centred redox pattern with the most intense anoxia in deep basinal areas. Although both systems exhibit large-scale estuarine circulation, the different redox patterns are due to differences in: (1) oxygen content of renewing deep waters (oxic in the Baltic, oxygen-deficient in the LPMS); (2) bathymetry (shallow sill and deep basins in the Baltic, lack of a shallow sill in the LPMS); and (3) geographic scale (greater distances of lateral

minimum zone (OMZ) expands considerably along the eastern tropical margins of oceans (Hay, 1995). In the eastern tropical Pacific, this expansion is due to a combination of enhanced, upwelling-driven productivity associated with easterly trade winds, a long watermass residence time occasioned by the failure of the subtropical anticyclones to penetrate this area, and the generally low dissolved oxygen content of Pacific seawater (Roden, 1964; Wyrtki, 1967; Ganeshram and Pedersen, 1998). Compared to typical depths of 500 to 1000 m, the upper surface of the eastern Pacific OMZ (as defined by the 1 mL L^{-1} dissolved oxygen isocon) shallows to <100 m from ~3°–12°S and ~5°–22°N latitude (Fig. 7; Levitus and Boyer, 1994). Because the entrance to the Late Pennsylvanian Greater Permian Basin Seaway was at ~5°–10°N paleolatitude, it is likely that shallowing of the paleo-OMZ in the eastern Panthalassic Ocean brought oxygen-depleted waters directly into the deep-water corridor leading to the LPMS (Heckel, 1977; Figs. 4, 8A; similarly, a shallowing of the Cretaceous OMZ was invoked as a factor controlling benthic anoxia in the Western Interior Basin by Arthur and Sageman, 2005). Second, 'preconditioning' of deep-waters reaching the LPMS was effected by benthic oxygen demand during the transit through the Greater Permian Basin Seaway. Intermediate-depth waters (~50–300 m deep) of the eastern Panthalassic Ocean entered the southwestern end of this seaway and flowed through a ~1000 km long deep-water corridor before reaching the LPMS (see above; Figs. 4–6; *cf*. Heckel, 1980). Although primary productivity levels and, therefore, benthic oxygen demand within the Greater Permian Basin region are unknown, the slow transit of waters through this corridor (~100 days at 0.1–0.2 m s^{-1}) allowed plenty of time for consumption of dissolved oxygen prior to lateral advection onto the Midcontinent Shelf (Figs. 8A, B). Among the epicontinental seas considered here, these processes are unique to the LPMS; Hudson Bay is the only modern epicontinental sea connected to the global ocean via an extended deep-water corridor (Hudson Strait), and strong tidal mixing within this corridor limits the potential for 'preconditioning' of the watermass entering this sea (Drinkwater, 1986).

From this analysis, we conclude that a unique set of boundary conditions and environmental dynamics resulted in the development of benthic anoxia across extensive portions of the LPMS during highstands. The key boundary conditions were: (1) extended orogenic highlands within the humid periequatorial region; (2) a largely landlocked setting; (3) shallow seafloor bathymetry; (4) an elongate, serpentine deep-water connection to the Panthalassic Ocean; and (5) location of the entrance of this deep-water corridor at 5–10°N paleolatitude, within a region of extreme shallowing of the paleo-oxygen minimum zone. Important environmental features resulting from these boundary conditions included: (1) a strong regional halocline, reducing vertical mixing; (2) limited volume of the subpycnoclinal watermass,

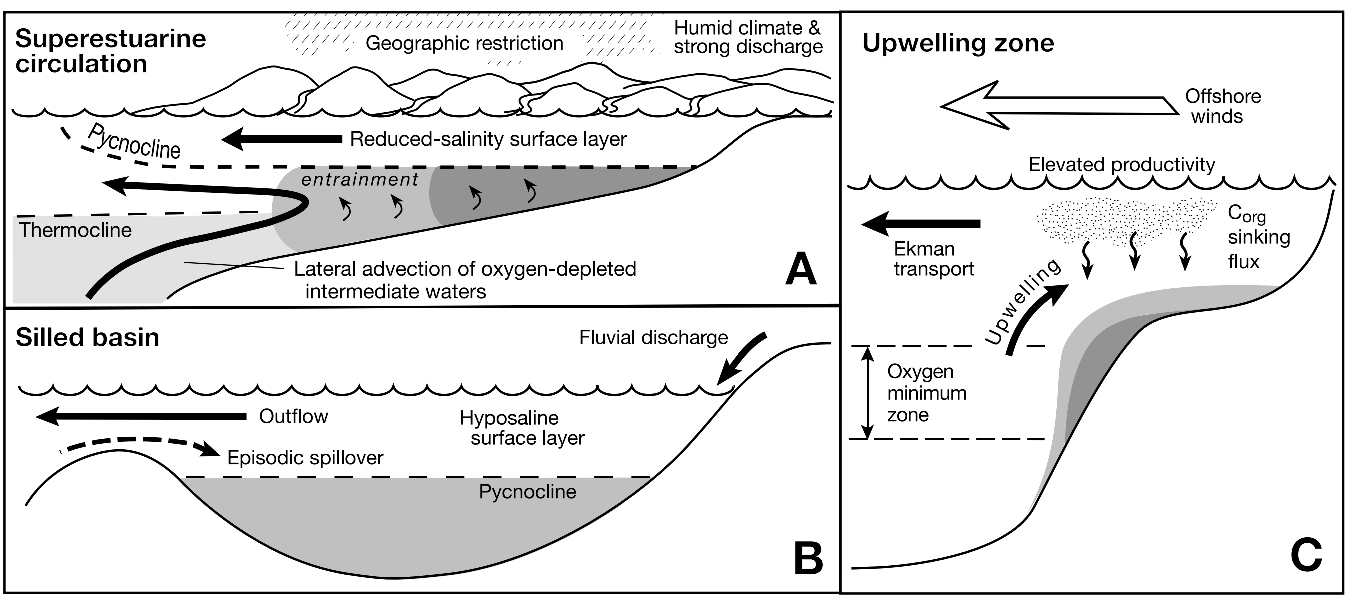

Figure 9. Models of marine anoxia, contrasting boundary conditions and environmental dynamics of (A) epicontinental-sea super-estuarine circulation systems *versus* (B) silled basins and (C) continental margin upwelling zones.

facilitating benthic oxygen depletion despite low primary productivity levels; and (3) the 'preconditioned', oxygen-deficient character of laterally advected deeper waters into the LPMS. This combination of boundary conditions and environmental responses does not exist in any of the large, modern epicontinental seas presently in existence.

SUPER-ESTUARINE CIRCULATION MODEL OF EPICONTINENTAL MARINE ANOXIA

Although depositional models for mid-continent cyclothemic core shales have been developed in a number of earlier studies (e.g., Heckel, 1977, 1980, 1991, 1994; Coveney et al., 1987; Hatch and Leventhal, 1992; Hoffman et al., 1998; Genger and Sethi, 1998; Algeo et al., 2004; Cruse and Lyons, 2004), our study offers the most detailed analysis of the environmental conditions and dynamics of the LPMS to date. Because our analysis demonstrates that the LPMS lacks a close modern analogue, we formalize its key characteristics by means of the *super-estuarine circulation model* of epicontinental marine anoxia, for which the LPMS may serve as the type example. This model can be considered a more detailed version of the quasi-estuarine circulation model for epicontinental seas put forth by Witzke (1987).

Super-estuarine marine environments are characterized by large-scale estuarine-type circulation on a broad, shallow and unsilled, or weakly silled, cratonic platform (Fig. 9A) While, modern estuaries exhibit several patterns of circulation, estuarine circulation denotes systems with major fluvial discharge and water-column stratification (e.g., Demaison and Moore, 1980; Kennish, 2001). The essential boundary conditions of this model are: (1) climatic humidity, which contributes to high river discharge, a broad, reduced-salinity surface-water layer, and a strong pycnocline; (2) geographic restriction, which limits lateral dispersion of the surface-water layer, tidal mixing, and deep-water renewal; (3) shallow seafloor bathymetry, which reduces the volume of the subpycnoclinal watermass, facilitating benthic oxygen depletion; and (4) geographic/climatic factors that precondition the source of the subpycnoclinal watermass to low-oxygen status. Large-scale estuarine-type circulation may be a necessary, but not a sufficient, condition for the development of widespread benthic anoxia in epicontinental seas, as shown by differences in redox conditions between the modern Baltic Sea and Hudson Bay. However, the absence of large-scale estuarine-type circulation is almost certain to preclude widespread benthic anoxia, as shown by the modern Gulf of Carpentaria.

The super-estuarine circulation model differs from the widely cited silled basin and continent-margin upwelling zone models for marine anoxia in terms of the key factors controlling benthic redox status. The key feature of the silled basin model is topographic restriction of deep-water exchange owing to existence of a shallow marginal sill (Fig. 9B), and that of the upwelling zone model is important vertical and/or lateral advection of nutrient-rich deep-waters with consequent increases in primary productivity and C_{org} sinking fluxes (Fig. 9C; Demaison and Moore, 1980; Wignall, 1994). Neither of these features was associated with the LPMS, which was characterized by a strong deep-water flux and by low levels of primary productivity. Rather, the key features of the *super-estuarine circulation model* for epicontinental marine anoxia are: (1) large-scale estuarine-type circulation and halocline formation; and (2) 'preconditioning' of the deep-water source to low-oxygen status beneath a thermocline. Although these features are present in some modern oxygen-deficient marine environments, they are not generally regarded as key elements of either the silled basin or the continental-margin upwelling-zone models for marine anoxia.

Super-estuarine marine systems potentially can be distinguished from silled basins and upwelling systems on the basis of characteristic patterns of compositional variation in sediments. Spatial variation in sediment composition reflects geographic variation in environmental conditions. Silled basins generally exhibit 'bulls-eye' patterns centred on the deepest and most anoxic portion of the water body, as in the modern Black Sea or Baltic Sea (Fig. 8C; Shimkus and Trimonis, 1974; Glasby et al., 1997). Continental-margin upwelling systems tend to exhibit patchy concentrations along a linear trend, reflecting local zones of upwelling (Reimers and Suess, 1981; Calvert and Price, 1983). By contrast, super-estuarine marine systems are characterized by fairly uniform spatial gradients in environmental conditions (e.g., pycnocline strength, benthic redox status) and, thus, sediment composition (Algeo and Maynard, 1997; Hoffman et al., 1998). Stratigraphic variation in sediment composition reflects the degree of temporal dynamism of a given environment. Silled basins tend to exhibit relatively stable watermass conditions owing to the basin-wide extent of their pycnoclines and the short-term immutability of key boundary conditions (e.g., sill depth) (Scranton et al., 1987; Murray, 1991). Continental-margin upwelling systems are generally highly dynamic at short time scales (i.e., months

movement of large, chemically variable watermasses along continental margins (Bailey and Chapman, 1991; Emeis et al., 1991); such systems can also exhibit systematic variation in environmental conditions at longer timescales (Ganeshram and Pedersen, 1998). Super-estuarine marine systems are intermediate in terms of their environmental dynamism. The existence of a strong pycnocline over large areas dampens temporal variability somewhat, relative to upwelling systems, but the 'open-ended' (i.e., laterally unconfined) character of pycnoclines in such systems makes them inherently more variable than pycnoclines in silled basins. Dependence of pycnocline strength and extent on climatic variables such as precipitation and fluvial runoff makes super-estuarine marine systems particularly susceptible to environmental fluctuations at intermediate time-scales (i.e., hundreds to tens of thousands of years). Detailed analysis of spatio-temporal patterns of compositional variation in the sediments of ancient marine systems should allow accurate discrimination among these contrasting environmental models.

CONCLUSIONS

Although modern epicontinental seas can provide insights regarding controls on benthic redox conditions, none represent a close analogue to the North American Late Pennsylvanian mid-continent Sea (LPMS). The LPMS was unique in developing strongly euxinic conditions over a large (~10^6 km^2) area of seafloor despite having a marginal sill too deep to restrict deep-water renewal and levels of primary productivity too low to impose a significant benthic oxygen demand. Rather, the key boundary conditions promoting widespread benthic anoxia in the LPMS were: (1) a humid paleoclimate; (2) a largely landlocked setting; (3) shallow seafloor bathymetry; (4) an elongate, tortuous deep-water connection to the global ocean; and (5) location of the entrance of this deep-water corridor in a region of extreme shallowing of the oxygen-minimum zone in the eastern Panthalassic Ocean. Important features of the LPMS environment deriving from these boundary conditions include: (1) a strong regional halocline, reducing vertical mixing of the water column; (2) limited volume of the subpycnoclinal watermass, facilitating benthic oxygen depletion despite low primary productivity; and (3) the 'preconditioned' oxygen-deficient status of laterally advected deeper waters beneath a thermocline. In contrast to the modern Baltic Sea, which exhibits a basin-centred pattern of benthic anoxia in accord with the silled basin model, the LPMS exhibits a strong lateral gradient in benthic redox conditions with development of the most intense anoxia in shallower interior regions of the sea. This pattern reflects the importance of large-scale estuarine circulation in a laterally unconfined epicontinental sea, representing a type of anoxic marine system herein designated the *super-estuarine circulation model*. Because benthic redox conditions in the LPMS were dependent on the strength and lateral extent of its pycnocline and, hence, on regional precipitation and fluvial discharge, the system was particularly sensitive to climate fluctuations at intermediate timescales (i.e., hundreds to thousands of years).

ACKNOWLEDGMENTS

We thank to Tim Phillips for drafting services, Lynn Watney, Lorenz Schwark and James Hower for helpful discussions, Bill Hay and an anonymous reviewer for constructive reviews of the manuscript and Brian Pratt for editorial help. This work was supported in part by a grant from the University of Cincinnati Research Council.

REFERENCES

Adams, J.E., Frenzel, H.N., Johnson, D.P. and Rhodes, M.L., 1951, Starved Pennsylvanian Midland Basin [Texas]: American Association of Petroleum Geologists Bulletin, v. 35, p. 2600–2607.

Algeo, T.J., 1992, Continent-scale wrenching of southwestern Laurussia during the Ouachita–Marathon Orogeny and tectonic escape of the Llano Block, *in* Lindsay, R.F. and Reed, C.L., eds., Sequence Stratigraphy Applied to Permian Basin Reservoirs: West Texas Geological Society, Publication 92–92, p. 115–131.

Algeo, T.J., 2004, Can marine anoxic events draw down the trace-element inventory of seawater?: Geology, v. 32, p. 1057–1060.

Algeo, T.J. and Lyons, T.W., 2006, Mo-TOC covariation in modern anoxic marine environments: Implications for analysis of paleo-redox and -hydrographic conditions: Paleoceanography, v. 21, PA1016,doi:10.10.1029/2004PA001112.

Algeo, T.J. and Maynard, J.B., 1997, Cyclic Sedimentation of Appalachian Devonian and Mid-continent Pennsylvanian Black Shales: Analysis of Ancient Anoxic Marine Systems—A Combined Core and Field Workshop: Joint Meeting of Eastern Section AAPG and The Society for Organic Petrography (TSOP), Lexington, Kentucky, Sept. 27–28, 1997, 147 p.

Algeo, T.J. and Maynard, J.B., 2004, Trace element behavior and redox facies in core shales of Upper Pennsylvanian Kansas-type cyclothems: Chemical Geology, v. 206, p. 289–318.

Algeo, T.J., Schwark, L. and Hower, J.C., 2004, High-resolution geochemistry and sequence stratigraphy of the Hushpuckney Shale (Swope Formation, eastern Kansas): Implications for climato-environmental dynamics of the Late Pennsylvanian Mid-continent Sea: Chemical Geology, v. 206, p. 259–288.

Alhonen, P., 1966, Baltic Sea, *in* Fairbridge, R.W., ed., The Encyclopedia of Oceanography: Reinhold, New York, p. 87–91.

Anderson, J.T. and Roff, J.C., 1980, Seston ecology of the surface-waters of Hudson Bay: Canadian Journal of Fisheries and Aquatic Sciences, v. 37, p. 2242–2253.

Anderson, T.F. and Pratt, L.M., 1995, Isotopic evidence for the origin of organic sulfur and elemental sulfur in marine sediments, *in* Vairavamurthy, M.A. and Schoonen, M.A.A., eds., Geochemical Transformations of Sedimentary Sulfur: American Chemical Society Symposium Series 612, Washington, D.C., p. 378–396.

Andrén, E., Andrén, T. and Sohlenius, G., 2000, The Holocene history of the southwestern Baltic Sea as reflected in a sediment core from the Bornholm Basin: Boreas, v. 29, p. 233–250.

Andrews, S. and Higgins, L.S., 1984, Influence of depositional facies on hydrocarbon production in the Tensleep Sandstone, Big Horn Basin, Wyoming: A working hypothesis, *in* Goolsby, J. and Morton, D., eds., The Permian and Pennsylvanian Geology of Wyoming, Wyoming Geological Association, 35th Annual Field Conference Guidebook, p. 183–197.

Arbenz, J.K., 1989, The Ouachita System, *in* Bally, A.W. and Palmer, A.R., eds., The Geology of North America—An Overview: Geological Society of America, The Geology of North America, v. A, p. 371–396.

Archer, A.W. and Greb, S.F., 1995, An Amazon-scale drainage system in the Early Pennsylvanian of central North America: Journal of Geology, v. 103, p. 611–627

Arthur, M.A. and Sageman, B.B., 1994, Marine black shales: Depositional mechanisms and environments of ancient deposits: Annual Review of Earth and Planetary Sciences, v. 22, p. 499–551.

Arthur, M.A. and Sageman, B.B., 2004, Sea-level control on source-rock development: perspectives from the Holocene Black Sea, the mid-Cretaceous Western Interior Basin of North America, and the Late Devonian Appalachian Basin, *in* Harris, N.B., eds., The Deposition of Organic-Carbon-Rich Sediments: Models, Mechanisms, and Consequences: SEPM (Society for Sedimentary Geology), Special Publication 82, p. 35–59.

Arthur, M.A., Dean, W.E., Neff, E.D., Hay, B.J., King, J. and Jones, G., 1994, Varve-calibrated records of carbonate and organic carbon accumulation over the last 2000 years in the Black Sea: Global Biogeochemical Cycles, v. 8, p. 195–217.

Bailey, G.W., 1991, Organic carbon flux and development of oxygen deficiency on the modern Benguela continental shelf south of 22°S: Spatial and temporal variability, *in* Tyson, R.V. and Pearson, T.H., eds., Modern and Ancient Continental Shelf Anoxia: Geological Society of London, Special Publication 58, p. 171–183.

Bailey, G.W. and Chapman, P., 1991, Short-term variability during an anchor station study in the southern Benguela upwelling system: Chemical and physical oceanography: Progress in Oceanography, v. 28, p. 9–37.

Barber, F.G., 1968, The water, *in* Beals, C.S., ed., Science, History and Hudson Bay, v. 1: Canada Department of Energy, Mines and Resources, Ottawa, p. 287–318.

Bianchi, T.S., Engelhaupt, E., Westman, P., Andrén, T., Rolff, C. and Elmgren, R., 2000, Cyanobacterial blooms in the Baltic Sea: Natural or human-induced?: Limnology and Oceanography, v. 45, p. 716–726.

Biksham, G. and d'Anglejan, B., 1989, Rate of sedimentation and geochemistry of southeastern Hudson Bay, Canada, *in* Hadley, R.F. and Ongley, E.D., eds., Sediment and the Environment: International Association of Hydrological Sciences, Publication 184, p. 27–36.

Björck, S., 1995, A review of the history of the Baltic Sea, 13.0–8.0 ka BP: Quaternary International, v. 27, p. 19–40.

Blakey, R.C., 2006, Carboniferous-Permian paleogeography of the assembly of Pangaea, *in* Wong, Th.E. (ed.): Proceedings of the 25th International Congress on Carboniferous and Permian Stratigraphy, Utrecht, 2003: Royal Dutch Academy of Arts and Sciences, Amsterdam.

Blakey, R.C., Peterson, F. and Kocurek, G., 1988, Synthesis of late Paleozoic and Mesozoic eolian deposits of the Western Interior of the United States: Sedimentary Geology, v. 56, p. 3–125.

Boardman, D.R. and Heckel, P.H., 1989, Glacial-eustatic sea-level curve for early Late Pennsylvanian sequence in north-central Texas and biostratigraphic correlation with curve for mid-continent North America: Geology, v. 17, p. 802–805.

Budnik, R.T., 1986, Left-lateral intraplate deformation along the Ancestral Rocky Mountains: Implications of late Paleozoic plate motions: Tectonophysics, v. 132, p. 195–214.

Budnik, R.T., 1989, Tectonic Structures of the Palo Duro Basin, Texas Panhandle: Texas Bureau of Economic Geology, Report of Investigations 187, 43 p.

Burchfiel, B.C., Cowan, D.S. and Davis, G.A., 1992, Tectonic overview of the Cordilleran orogen in the western United States, *in* Burchfiel, B.C., Lipman, P.W. and Zoback, M.L., eds., The Cordilleran Orogen: Conterminous U.S.: Geological Society of America, The Geology of North America, v. G-3, p. 407–479.

Calvert, S.E. and Price, N.B., 1983, Geochemistry of Namibian Shelf sediments, *in* Suess, E. and Thiede, J., eds., Coastal Upwelling: Its Sediment Record, pt. A: Responses of the Sedimentary Regime to Present Coastal Upwelling: Plenum, New York, p. 337–375.

Campbell, N.J., 1958, The oceanography of Hudson Strait: Fisheries Research Board of Canada, Mans. Rep. Ser. 12, 60 p.

Canfield, D.E., 1994, Factors influencing organic carbon preservation in marine sediments: Chemical Geology, v. 114, p. 315–329.

Casey, J.M., 1980, Depositional systems and paleogeographic

Mexico, *in* Fouch, T.D. and Magathan, E.R., eds., Paleozoic Paleogeography of the West-central United States: SEPM Rocky Mountain Section, Denver, Colorado, p. 181–196.

Cecil, C.B., 1990, Paleoclimate controls on stratigraphic repetition of chemical and siliciclastic rocks: Geology, v. 18, p. 533–536.

Cecil, C.B., Dulong, F.T., Edgar, N.T., Stamm, R.G., Wardlaw, B.R. and West, R.R., 2003b. Climate controls on the stratigraphy of a Middle Pennsylvanian cyclothem in North America, *in* Cecil, C.B. and Edgar, N.T., eds., Climate Controls on Stratigraphy: SEPM (Society for Sedimentary Geology), Special Publication 77, p. 151–180.

Cecil, C.B., Dulong, F.T., Harris, R.A., Cobb, J.C., Gluskoter, H.G. and Nugroho, H., 2003a, Observations on climate and sediment discharge in selected tropical rivers, Indonesia, *in* Cecil, C.B. and Edgar, N.T., eds., Climate Controls on Stratigraphy: SEPM (Society for Sedimentary Geology), Special Publication 77, p. 29–50.

Chester, R., 1990, Marine Geochemistry: Unwin Hyman, London, 698 p.

Church, J.A. and Forbes, A.M.G., 1981, Non-linear model of the tides in the Gulf of Carpentaria: Australian Journal of Marine and Freshwater Research, v. 32, p. 685–697.

Collin, A.E., 1966, Hudson Bay and approaches, Part A. Introduction and oceanography, *in* Fairbridge, R.W., ed., The Encyclopedia of Oceanography: Reinhold, New York, p. 357–359.

Cook, T.D. and Bally, A.W., 1975, Stratigraphic Atlas of North and Central America: Princeton University Press, Princeton, 272 p.

Coveney, R.M., Leventhal, J.S., Glascock, M.D. and Hatch, J.R., 1987, Origins of metals and organic matter in the Mecca Quarry Shale Member and stratigraphically equivalent beds across the Midwest: Economic Geology, v. 82, p. 915–933.

Coveney, R.M., and Shaffer, N.R., 1988, Sulfur-isotope variations in Pennsylvanian shales of the midwestern United States: Geology, v. 16, p. 18–21.

Coveney, R.M., Watney, W.L. and Maples, C.G., 1991, Contrasting depositional models for Pennsylvanian black shale discerned from molybdenum abundances: Geology, v. 19, p. 147–150.

Crowley, T.J. and Baum, S.K., 1991, Estimating Carboniferous sea-level fluctuations from Gondwanan ice extent: Geology, v. 19, p. 975–977.

Crowley, T.J., Hyde, W.T. and Short, D.A., 1989, Seasonal cycle variations on the supercontinent of Pangaea: Geology, v. 17, p. 457–460.

Crowley, T.J., Yip, K.-J., Baum, S.K. and Moore, S.B., 1996, Modelling Carboniferous coal formation: Paleoclimates, v. 2, p. 159–177.

Cruse, A.M. and Lyons, T.W., 2004, Trace metal records of regional paleoenvironmental variability in Pennsylvanian (Upper Carboniferous) black shales: Chemical Geology, v. 206, p. 319–345.

Cys, J.M. and Gibson, W.R., 1988, Pennsylvanian and Permian geology of the Permian Basin region, *in* Sloss, L.L., ed., Sedimentary Cover—North American Craton: U.S.: Geological Society of America, The Geology of North America, v. D-2, p. 277–289.

De Deckker, P., Chivas, A.R., Shelley, J.M.G. and Torgersen, T., 1988, Ostracod shell chemistry: A new palaeoenvironmental indicator applied to a regressive/transgressive record from the Gulf of Carpentaria, Australia: Palaeogeography Palaeoclimatology Palaeoecology, v. 66, p. 231–241.

Demaison, G.J. and Moore, G.T., 1980, Anoxic environments and oil source bed genesis: American Association of Petroleum Geologists Bulletin, v. 64, p. 1179–1209.

Desmond, R.J., Steidtmann, J.R. and Cardinal, D.F., 1984, Stratigraphy and depositional environments of the Middle Member of the Minnelusa Formation, central Powder River Basin, Wyoming, *in* Goolsby, J. and Morton, D., eds., The Permian and Pennsylvanian Geology of Wyoming, Wyoming Geological Association, 35th Annual Field Conference Guidebook, p. 213–239.

Dickinson, W.R. and Lawton, T.F., 2001, Carboniferous to Cretaceous assembly and fragmentation of Mexico: Geological Society of America Bulletin, v. 113, p. 1142–1160.

Dickinson, W.R., Patchett, P.J., Ferguson, C.A., Suneson, N.H. and Gleason, J.D., 2003, Nd isotopes of Atoka Formation (Pennsylvanian) turbidites displaying anomalous east-flowing paleocurrents in the frontal Ouachita Belt of Oklahoma: Implications for regional sediment dispersal: Journal of Geology, v. 111, p. 733–740.

DiMichele, W.A. and Phillips, T.L., 1996, Climate change, plant extinctions, and vegetational recovery during the Middle–Late Pennsylvanian transition: The case of tropical peat-forming environments in North America, *in* Hart, M.L., ed., Biotic Recovery From Mass Extinctions: Geological Society of London, Special Publication 102, p. 201–221.

Doutch, H.F., 1976, Carpentaria Basin, *in* Leslie, R.B., Evans, H.J. and Knight, C.L., eds., Economic Geology of Australia and Papua New Guinea, v. 3, Petroleum: Australasian Institute of Mining and Metallurgy, Parkville, Victoria, p. 374–379.

Drever, J.I., 1988, The Geochemistry of Natural Waters [2nd edn.]: Prentice-Hall, Englewood Cliffs, New Jersey, 437 p.

Driese, S.G. and Dott, R.H., 1984, Model for sandstone-carbonate "cyclothems" based on upper member of Morgan Formation (Middle Pennsylvanian) of Northern Utah and Colorado: American Association of Petroleum Geologists Bulletin, v. 68, p. 574–597.

Drinkwater, K.F., 1986, Physical oceanography of Hudson Strait and Ungava Bay, *in* Martini, I.P.., ed., Canadian Inland Seas: Oceanography Series 44, Elsevier Amsterdam, p. 237–264.

Dybern, B.I. and Fonselius, S.H., 1981, Pollution, *in* Voipio, A.V., ed., The Baltic Sea: Oceanography Series 30, Elsevier, Amsterdam, p. 351–381.

Dyrssen, D., Hall, P., Haraldsson, C., Iverfeldt, Å. and Westerlund, S., 1984, Trace metal concentrations in the anoxic bottom-water of Framvaren, *in* Kramer, C.J.M. and Duinker, J.C., eds., Complexation of Trace Metals in Natural Waters: Martinus Nijhoff/Dr. W. Junk Publishers, The Hague, p. 239–243.

Edgar, N.T., Cecil, C.B., Mattick, R.E., Chivas, A.R., De Deckker, P. and Djajadihardja, Y.S., 2003, A modern analogueue for tectonic, eustatic, and climatic processes in cratonic basins: Gulf of Carpentaria, northern Australia, *in* Cecil, C.B. and Edgar, N.T., eds., Climate Controls on Stratigraphy: SEPM (Society for Sedimentary Geology), Special Publication 77, p. 193–205.

Ehlin, U., 1981, Hydrology of the Baltic Sea, *in* Voipio, A.V., ed., The Baltic Sea: Oceanography Series 30, Elsevier, Amsterdam, p. 123–134.

Emeis, K.-C., Whelan, J.K. and Tarafa, M., 1991, Sedimentary and geochemical expressions of oxic and anoxic conditions on the Peru Shelf, *in* Tyson, R.V. and Pearson, T.H., eds., Modern and Ancient Continental Shelf Anoxia: Geological Society, Special Publication 58, p. 155–170.

Emeis, K.-C., Larsen, B. and Seibold, E., 1992, What is the environmental capacity of enclosed marginal seas? Approaches to the problem in the Baltic, North, and Mediterranean Seas, *in* Hsü, K.J. and Thiede, J., eds., Use and Misuse of the Seafloor: Wiley, New York, p. 181–211.

Fahrer, T.R., 1996, Stratigraphy, petrography and paleoecology of marine units within the Conemaugh Group (Upper Pennsylvanian) of the Appalachian Basin in Ohio, West Virginia and Pennsylvania. unpub. Ph.D. thesis, University of Iowa, Iowa City, 298 p.

Faill, R.T., 1997, A geologic history of the north-central Appalachians; Part 2, The Appalachian Basin from the Silurian through the Carboniferous: American Journal of Science, v. 297, p. 729–761.

Fanshawe, J.R., 1978, Central Montana tectonics and the Tyler Formation, *in* Estelle, D. and Miller, R., eds., 1978 Williston Basin Symposium: Montana Geological Society, 24th Annual Conference, Billings, Montana, p. 239–248.

Feldman, H.R., Franseen, E.K., Joeckel, R.M. and Heckel, P.H., 2005, Impact of longer-term modest climate shifts on architecture of high-frequency sequences (cyclothems), Pennsylvanian of Mid-continent USA: Journal of Sedimentary Research, v. 75, p. 354–372.

Filippelli, G.M., 1997, Controls on phosphorus concentration and accumulation in oceanic sediments: Marine Geology, v. 139, p. 231–240.

Föllmi, K.B., 1996, The phosphorus cycle, phosphogenesis and marine phosphate-rich deposits: Earth-Science Reviews, v. 40, p. 55–124.

Forbes, A.M.G., 1984, The contribution of local processes to the seasonal hydrology of the Gulf of Carpentaria: Oceanographie Tropicale, v. 19, p. 193–201.

Friedrich, H., 1969, Marine Biology: Sidgwick & Jackson, London, 474 p.

Ganeshram, R.S. and Pedersen, T.F., 1998, Glacial–interglacial variability in upwelling and bioproductivity off NW Mexico: implications for Quaternary paleoclimate: Paleoceanography, v. 13, p. 634–645.

Garfield, T.R., Scott, A.J. and Walker, A.L., 1988, Overview: Late Paleozoic geologic history of the northern Denver Basin, *in* Goolsby, S.M. and Longman, M.W., eds., Occurrence and Petrophysical Properties of Carbonate Reservoirs in the Rocky Mountain Region: Rocky Mountain Association of Geologists, Denver, Colorado, p. 1–18.

Genger, D. and Sethi, P., 1998, A geochemical and sedimentological investigation of high-resolution environmental changes within the Late Pennsylvanian (Missourian) Eudora core black shale of the Mid-Continent region, U.S.A., *in* Schieber, J., Zimmerle, W. and Sethi, P.S., eds., Shales and Mudstones, v. 1.: Schweizerbart, Stuttgart, p. 271–293.

Geslin, J.K., 1998, Distal Ancestral Rocky Mountains tectonism: Evolution of the Pennsylvanian–Permian Oquirrh–Wood River basin, southern Idaho: Geological Society of America Bulletin, v. 110, p. 644–663.

Gibling, M.R., Calder, J.H., Ryan, R., van de Poll, H.W. and Yeo, G.M., 1992, Late Carboniferous and early Permian drainage patterns in Atlantic Canada: Canadian Journal of Earth Sciences, v. 29, p. 338–352.

Glasby, G.P., Emelyanov, E.M., Zhamoida, V.A., Baturin, G.N., Leipe, T., Bahlo, R. and Bonacker, P., 1997, Environments of formation of ferromanganese concretions in the Baltic Sea: a critical review, *in* Nicholson, K., Hein, J.R., Bühn, B. and Dasgupta, S., eds., Manganese Mineralization: Geochemistry and Mineralogy of Terrestrial and Marine Deposits: Geological Society, Special Publication, v. 119, p. 213–237.

Glenn, C.R. and 15 others, 1994, Phosphorus and phosphorites: Sedimentology and environments of formation: Eclogae Geologicae Helvetiae, v. 87, p. 747–788.

Goldstein, S.J. and Jacobsen, S.B., 1988, REE in the Great Whale River estuary, Northwest Quebec: Earth and Planetary Science Letters, v. 88, p. 241–252.

Grasshoff, K. and Voipio, A., 1981, Chemical oceanography, *in* Voipio, A.V., ed., The Baltic Sea: Oceanography Series 30, Elsevier, Amsterdam, p. 183–218.

Greb, S.F., Andrews, W.M., Cecil, C.B., DiMichele, W., Eble, C.F. and Hower, J.C., 2003, Desmoinesian coal beds of the Eastern Interior and surrounding basins; the largest tropical peat mires in Earth history, *in* Chan, M.A., ed., Extreme Depositional Eenvironments; Mega End Members in Geologic Time: Geological Society of America, Special Publication 370, p. 127–150.

Hällfors, G., Niemi, A., Ackefors, H., Lassig, J. and Leppäkoski, E., 1981, Biological oceanography, Voipio, A.V., ed., The Baltic Sea: Oceanography Series 30, Elsevier, Amsterdam, p. 219–274.

Hamlin, H.S., Clift, S.J., Dutton, S.P., Hentz, T.F. and Laubach, S.E., 1995, Canyon Sandstones—A Geologically Complex Natural Gas Play in Slope and Basin Facies, Val Verde Basin, Southwest Texas: Texas Bureau of Economic Geology, Report of Investigations 232, 74 p.

Handford, C.R. and Dutton, S.P., 1980, Pennsylvanian–Early Permian depositional systems and shelf-margin evolution, Palo Duro Basin, Texas: American Association of Petroleum Geologists Bulletin, v. 64, p. 88–106.

Handford, C.R., Dutton, S.P. and Fredericks, P.E., 1981, Regional Cross Sections of the Texas Panhandle: Precambrian to Mid-Permian: Texas Bureau of Economic Geology, 8 p.

Handford, C.R. and Fredericks, P.E., 1980, Lower Permian Facies of the Palo Duro Basin, Texas: Depositional Systems, Shelf-margin Evolution, Paleogeography, and Petroleum Potential: Texas Bureau of Economic Geology, Report of Investigations 102, 31 p.

Hatch, J.R. and Leventhal, J.S., 1992, Relationship between inferred redox potential of the depositional environment and geochemistry of the Upper Pennsylvanian (Missourian) Stark Shale Member of the Dennis Limestone, Wabaunsee County, Kansas, U.S.A.: Chemical Geology, v. 99, p. 65–82.

Hay, W.W., 1995, Paleoceanography of marine organic-carbon-rich sediments, *in* Huc, A.-Y., ed., Paleogeography, Paleoclimate, and Source Rocks: American Association of Petroleum Geologists, Studies in Geology 40, p. 21–59.

Hay, W.W., Wold, C.N., Söding, E. and Flögel, S., 2001, Evolution of sediment fluxes and ocean salinity, *in* Merriam, D.F. and Davis, J.C., eds., Geologic Modeling and Simulation: Sedimentary Systems: Kluwer Academic/Plenum, New York, p. 153–167.

Hay, W.W., Migdisov, A., Balukhovsky, A.N., Wold, C.N., Flögel, S. and Söding, E., 2006, Evaporites and the salinity of the ocean during the Phanerozoic: implications for climate, ocean circulation and life: Palaeogeography, Palaeoclimatology Palaeoecology, v. 240, p. 3–46.

Heckel, P.H., 1977, Origin of phosphatic black shale facies in Pennsylvanian cyclothems of mid-contintent North America: American Association of Petroleum Geologists Bulletin, v. 61, p. 1045–1068.

Heckel, P.H., 1980, Paleogeography of eustatic model for deposition of Mid-continent Upper Pennsylvanian cyclothems, *in* Fouch, T.D. and Magathan, E.R., eds., Paleozoic Paleogeography of the West-central United States: SEPM, Rocky Mountain Section, Denver, Colorado, p. 197–215.

Heckel, P.H., 1986, Sea-level curve for Pennsylvanian eustatic marine transgressive-regressive depositional cycles along mid-continent outcrop belt, North America: Geology, v. 14, p. 330–334.

Heckel, P.H., 1991, Thin widespread Pennsylvanian black shales of Midcontintent North America: A record of a cyclic succession of widespread pycnoclines in a fluctuating epeiric sea, *in* Tyson, R.V. and Pearson, T.H., eds., Modern and Ancient Continental Shelf Anoxia: Geological Society, Special Publication 58, p. 259–273.

Heckel, P.H., 1994, Evaluation of evidence for glacial-eustatic control over marine Pennsylvanian cyclothems in North America and consideration of possible tectonic effects, *in* Dennison, J.M. and Ettensohn, F.R., eds., Tectonic and Eustatic Controls on Sedimentary Cycles: SEPM, Concepts in Sedimentology and Paleontology 4, p. 65–87.

Heckel, P.H., 1995, Glacial-eustatic base-level climatic model for late Middle to Late Pennsylvanian coal-bed formation in the Appalachian Basin: Journal of Sedimentary Research, v. B65, p. 348–356.

Heckel, P.H., 2002, Overview of Pennsylvanian cyclothems in Mid-continent North America and brief summary of those elsewhere in the World, *in* Hills, L.V., Henderson, C.V. and Bamber, E.W., eds., Carboniferous and Permian of the World: Canadian Society of Petroleum Geologists, Memoir 19, p. 79–98.

Heckel, P.H., 2004, Updated cyclothem grouping chart and observations on the grouping of Pennsylvanian cyclothems in Mid-continent North America: Newsletter on Carboniferous Stratigraphy, v. 22, p. 18–22.

Heckel, P.H. and Baesemann, J.M., 1975, Environmental interpretation of conodont distribution in Upper Pennsylvanian (Missourian) megacyclothems in eastern Kansas: American Association of Petroleum Geologists Bulletin, v. 59, p. 486–509.

Heckel, P.H. and Hatch, J.R., 1992, Comment on "Contrasting depositional models for Pennsylvanian black shale discerned from molybdenum abundances" by R.M. Coveney et al.: Geology, v. 20, p. 88–89.

HELCOM, 1996, Third periodic assessment of the state of the marine environment of the Baltic Sea, 1989–1993: Helsinki Commission, Baltic Sea Environment Proceedings, 69 p.

Hill, C.A., 1999, Reevaluation of the Hovey Channel in the Delaware Basin, West Texas: American Association of Petroleum Geologists Bulletin, v. 83, p. 277–294.

Hoffman, D.L., Algeo, T.J., Maynard, J.B., Joachimski, M.M., Hower, J.C. and Jaminski, J., 1998, Regional and stratigraphic variation in bottom-water anoxia in offshore core shales of Upper Pennsylvanian cyclothems from the Eastern Mid-continent Shelf (Kansas), USA, *in* Schieber, J., Zimmerle, W. and Sethi, P.S., eds., Shales and Mudstones, v. 1: Schweizerbart, Stuttgart, p. 243–269.

Hoy, R.G. and Ridgway, K.D., 2002, Syndepositional thrust-related deformation and sedimentation in an Ancestral Rocky Mountains basin, Central Colorado trough, Colorado, USA: Geological Society of America Bulletin, v. 114, p. 804–828.

Hydrological Atlas of Canada, 1978, Canadian Department of Fisheries and Environment, Ottawa, Canada, Publication EN 37-26/1978, Map 22.

Jackson, W.E., 1964, Depositional topography and cyclic deposition in west-central Texas: American Association of Petroleum Geologists Bulletin, v. 48, p. 317–328.

Jennings, J.N., 1972, Some attributes of Torres Strait, in Walker, D., ed., Bridge and Barrier: The Natural and Cultural History of Torres Strait: Australian National University, Department of Biogeography and Geomorphology, Publication BG/3, p. 29–38.

Joachimski, M.M., von Bitter, P.H. and Buggisch, W., 2006, Constraints on Pennsylvanian glacioeustatic sea-level changes using oxygen isotopes of conodont apatite: Geology, v. 34, p. 277–280.

Joeckel, R.M., 1994, Virgilian (Upper Pennsylvanian) paleosols in the Upper Lawrence Formation (Douglas Group) and in the Snyderville Shale Member (Oread Formation, Shawnee Group) of the northern Mid-continent, USA: Pedologic contrasts in a cyclothem sequence: Journal of Sedimentary Research, v. A64, p. 853–866.

Joeckel, R.M., 1999, Paleosol in Galesburg Formation (Kansas City Group, Upper Pennsylvanian), northern Mid-continent, U.S.A.: Evidence for climate change and mechanisms of marine transgression: Journal of Sedimentary Research, v. 69, p. 720–737.

Jones, M.R., 1987, Surficial sediments of the western Gulf of Carpentaria, Australia: Australian Journal of Marine and Freshwater Research, v. 38, p. 151–167.

Jones, M.R. and Torgersen, T., 1988, Late Quaternary evolution of Lake Carpentaria on the Australia–New Guinea continental shelf: Australian Journal of Earth Sciences, v. 35, p. 313–324.

Jongsma, D., 1974, Marine Geology of the Arafura Sea: Australian Bureau of Mineral Resources, Geology and Geophysics, Bulletin 157, 73 p.

Jonsson, P., Carman, R. and Wulff, F., 1990, Laminated sediments in the Baltic—a tool for evaluating nutrient mass balances: Ambio, v. 19, p. 152–158.

Karhu, M., Horstmann, U. and Rud, O., 1994, Satellite detection of increased cyanobacteria in the Baltic Sea: Natural fluctuation or ecosystem change?: Ambio, v. 23, p. 469–472.

Karl, D. M. and Knauer, G.A., 1991, Microbial production and particle flux in the upper 350 m of the Black Sea: Deep-Sea Research, v. A38, p. S921–S942.

Kennett, J., 1982, Marine Geology: Prentice-Hall, Englewood Cliffs, New Jersey, 813 p.

Kennish, M.J., ed., 2001, Practical Handbook of Marine Science [3rd edn.]: CRC Press, Boca Raton, Florida, 876 p.

Kerr, D.R. and Dott, R.H., 1988, Eolian dune types preserved in the Tensleep Sandstone (Pennsylvanian–Permian), north-central Wyoming: Sedimentary Geology, v. 56, p. 383–402.

Kidder, D.L., 1985, Petrology and origin of phosphatic nodules from the mid-continent Pennsylvanian epicontinental sea: Journal of Sedimentary Petrology, v. 55, p. 809–816.

Kidder, D.L., Hussein, R.A.M., Mapes, R.H. and Eddy-Dilek, C.A., 1996, Regional diagenetic variation in maximum-transgression phosphates from Mid-continent Pennsylvanian shales, *in* Witzke, B.J., Ludvigson, G.A. and Day, J., eds., Paleozoic Sequence Stratigraphy: Views from the North American Craton: Geological Society of America, Special Paper 306, p. 351–358.

Kluth, C.J., 1986, Plate tectonics of the Ancestral Rocky Mountains, *in* Peterson, J.A., ed., Paleotectonics and Sedimentation in the Rocky Mountain Region, United States: American Association of Petroleum Geologists, Memoir 41, p. 353–369.

Kluth, C.F., 1998, Discussion of "Late Paleozoic deformation of interior North America: The greater Ancestral Rocky Mountains": American Association of Petroleum Geologists Bulletin, v. 82, p. 2272–2276.

Kluth, C.F. and Coney, P.J., 1981, Plate tectonics of the Ancestral Rocky Mountains: Geology, v. 9, p. 10–15.

Knauth, L.P., 1998. Salinity history of the Earth's early history: Nature, v. 395, p. 554.

Kullenberg, G., 1981, Physical oceanography, *in* Voipio, A.V., ed., The Baltic Sea: Oceanography Series 30, Elsevier, Amsterdam, p. 135–183.

Landis, C.R., Trabelsi, A. and Strathearn, G., 1992, Hydrocarbon potential of selected Permian Basin shales as classified within the organic facies concept, *in* Johnson, K.S. and Cardott, B.J., eds., Source Rocks in the Southern Mid-continent, 1990 Symposium: Oklahoma Geological Survey Circular 93, p. 229–247.

Larsson, U., Elmgren, R. and Wulff, F., 1985, Eutrophication and the Baltic Sea: Causes and consequences: Ambio, v. 14, p. 9–14.

Lass, H.U. and Matthäus, W., 1996, On temporal wind variations forcing salt water inflows into the Baltic Sea: Tellus, v. A48, p. 663–671.

Lemke, W. and Kuijpers, A., 1995, Late Pleistocene and Early Holocene paleogeography of the Darss Sill area, southwestern Baltic: Quaternary International, v. 27, p. 73–81.

Lemke, W., Jensen, J.B., Bennike, O., Endler, R., Witkowski, A. and Kuijpers, A., 2001, Hydrographic thresholds in the western Baltic Sea: Late Quaternary geology and the Dana River concept: Marine Geology, v. 176, p. 191–201.

Leslie, R.J., 1964, Sedimentology of Hudson Bay, District of Keewatin, 34, 44, and 54: Geological Survey of Canada, Paper 63–48, 31 p.

Levitus, S. and Boyer, T., 1994, World Ocean Atlas 1994, Volume 2: Oxygen. NOAA Atlas NESDIS 2, U.S. Department of Commerce, Washington, D.C. (http://iridl.ldeo.columbia.edu/sources/.levitus94/.annual/.O2/)

Long, B.G. and Poiner, I.R., 1994, Infaunal benthic community structure and function in the Gulf of Carpentaria, northern Australia: Australian Journal of Marine and Freshwater Research, v. 45, p. 293–316.

Ludwig, W. and Probst, J.-L., 1998, River sediment discharge to the oceans: Present-day controls and global budgets: American Journal of Science, v. 298, p. 265–295.

Luebking, G.A., Longman, M.W. and Carlisle, W.J., 2001, Unconformity-related chert/dolomite production in the Pennsylvanian Amsden Formation, Wolf Springs fields, Bull Mountains basin of central Montana: American Association of Petroleum Geologists Bulletin, v. 85, p. 131–148.

Lyons, T.W., 1991, Upper Holocene sediments of the Black Sea: Summary of Leg 4 box cores (1988 Black Sea Oceanographic Expedition), *in* Izdar, E. and Murray, J.W., eds., Black Sea Oceanography: Kluwer, Dordrecht, p. 401–441.

Malinky, J.M. and Heckel, P.H., 1998, Paleoecology and taphonomy of faunal assemblages in grey core (offshore) shales in Mid-continent Pennsylvanian cyclothems: Palaios, v. 13, p. 311–334.

Manheim, F.T., 1961, A geochemical profile in the Baltic Sea: Geochimica et Cosmochimica Acta, v. 25, p. 52–70.

Mankiewicz, D. and Steidtmann, J.R., 1979, Depositional environments and diagenesis of the Tensleep Sandstone: eastern Big Horn Basin, Wyoming, *in* Scholle, P.A., ed., Aspects of Diagenesis: Society of Economic Paleontologists and Mineralogists, Special Publication 26, p. 319–336.

Marlow, J.R., Lange, C.B., Wefer, G. and Rosell-Melé, A., 2000, Upwelling intensification as part of the Pliocene–Pleistocene climate transition: Science, v. 290, p. 2288–2291.

Martini, I.P., 1986, Coastal features of Canadian Inland Seas, *in* Martini, I.P., ed., Canadian Inland Seas: Oceanography Series 44, Elsevier, Amsterdam, p. 117–142.

Matthäus, W., 1995, Natural variability and human impacts reflected in long-term changes in the Baltic deep-water conditions—a brief review: Deutsche Hydrographische Zeitschrift, v. 47, p. 47–65.

Maughan, E.K., 1984, Paleogeographic setting of Pennsylvanian Tyler Formation and relation to underlying Mississippian rocks in Montana and North Dakota: American Association of Petroleum Geologists Bulletin, v. 68, p. 178–195.

Maughan, E.K., 1993, The Ancestral Rocky Mountains in Wyoming, *in* Snoke, A.W., Steidtmann, J.R. and Roberts, S.M., eds., Geology of Wyoming: Geological Survey of Wyoming, Memoir 5, p. 188–207.

Maxwell, J.B., 1986, A climate overview of the Canadian Inland Seas, *in* Martini, I.P., ed., Canadian Inland Seas: Oceanography Series 44, Elsevier, Amsterdam, p. 79–99.

McKee, E.D. and 14 others, 1975, Paleotectonic Investigations of the Pennsylvanian System in the United States: U.S. Geological Survey Professional Paper 853, 541 p.

Miller, E.L., Miller, M.M., Stevens, C.H., Wright, J.E. and Madrid, R., 1992, Late Paleozoic paleogeography and tectonic evolution of the western U.S. Cordillera, *in* Burchfiel, B.C., Lipman, P.W. and Zoback, M.L., eds., The Cordilleran Orogen: Conterminous U.S.: The Geology of North America, v. G-3, Geological Society of America, p. 57–106.

Milliman, J.D. and Syvitski, J.P.M., 1992, Geomorphic/tectonic control of sediment discharge to the ocean: the importance of small mountainous rivers: Journal of Geology, v. 100, p. 525–544.

Mitrovica, J.X., Forte, A.M. and Simons, M., 2000, A reappraisal of postglacial decay times from Richmond Gulf and James Bay, Canada: Geophysical Journal International, v. 142, p. 783–800.

Murray, J.W., 1991, Hydrographic variability in the Black Sea, *in* Izdar, E. and Murray, J.W., eds., Black Sea Oceanography: Kluwer, Dordrecht, p. 1–16.

Nausch, G., Matthäus, W. and Feistel, R., 2003, Hydrographic and hydrochemical conditions in the Gotland Deep area between 1992 and 2003: Oceanologia, v. 45, p. 557–569.

Newell, B.S., 1973, Hydrology of the Gulf of Carpentaria, Australia: Commonwealth Scientific and Industrial Research Organization (CSIRO), Division of Fisheries and Oceanography, Technical Paper 35, 29 p.

Niemi, Å., 1979, Blue-green algal blooms and N:P ratio in the Baltic Sea: Acta Botanica Fennica, v. 110, p. 57–61.

Norris, A.W., 1993, Hudson Platform—Introduction, *in* Stott, D.F. and Aitken, J.D., eds., Sedimentary Cover of the Craton in Canada: Geological Survey of Canada, Geology of Canada, 5, p. 643–651; also Geological Society of America, The Geology of North America, v. D-1.

Parrish, J.T., 1993, Climate of the supercontinent Pangea: Journal of Geology, v. 101, p. 215–233.

Parrish, J.T. and Peterson, F., 1988, Wind directions predicted from global circulation models and wind directions determined from eolian sandstones of the western United States—A comparison: Sedimentary Geology, v. 56, p. 261–282.

Pelletier, B.R., 1986, Seafloor morphology and sediments, *in* Martini, I.P., ed., Canadian Inland Seas: Oceanography Series 44, Elsevier, Amsterdam, p. 143–162.

Pelletier, B.R., Wagner, F.J.E. and Grant, A.C., 1968, Marine geology, *in* Beals, C.S., ed., Science, History and Hudson Bay, v. 2: Canada Department of Energy, Mines and Resources, Ottawa, p. 557–613.

Peterson, J.A. and MacCary, L.M., 1987, Regional stratigraphy and general petroleum geology of the U.S. portion of the Williston Basin and adjacent areas, *in* Longman, M.W., ed., Williston Basin: Anatomy of a Cratonic Oil Province: Rocky Mountain Association of Geologists, Denver, Colorado, p. 9–43.

Pett, R.J. and Roff, J.C., 1982, Some observations and deductions concerning the deep-waters of Hudson Bay: Naturaliste Canadien, v. 109, p. 767–774.

Porter-Smith, R., Harris, P.T., Andersen, O.B., Coleman, R., Greenslade, D. and Jenkins, C.J., 2004, Classification of the Australian continental shelf based on predicted sediment threshold exceedance from tidal currents and swell waves: Marine Geology, v. 211, p. 1–20.

Prinsenberg, S.J., 1986, Salinity and temperature distributions of Hudson Bay and James Bay, *in* Martini, I.P., ed., Canadian Inland Seas: Oceanography Series 44, Elsevier, Amsterdam, p. 163–186.

Prinsenberg, S.J. and Freeman, N.G., 1986, Tidal heights and currents in Hudson Bay and James Bay, *in* Martini, I.P., ed., Canadian Inland Seas: Oceanography Series 44, Elsevier, Amsterdam, p. 205–216.

Quandt, L.R., 1990, Depositional environments and sandstone diagenesis in the Tyler Formation (Pennsylvanian), western North Dakota: Unpublished M.Sc. thesis, University of North Dakota, Grand Forks, North Dakota, 278 p.

Raffaelli, D.G., 1996, Intertidal Ecology: Chapman & Hall, New York, 356 p.

Reimers, C.E. and Suess, E., 1991, Spatial and temporal patterns of organic matter accumulation on the Peru continental margin, *in* Thiede, J. and Suess, E., eds., Coastal Upwelling: Its Sediment Record, pt. B: Sedimentary Records of Ancient Coastal Upwelling: Plenum, New York, p. 311–345.

Rochford, D.J., 1966, Some hydrological features of the eastern Arafura Sea and the Gulf of Carpentaria in August 1964: Australian Journal of Marine and Freshwater Research, v. 17, p. 31–60.

Roden, G.I., 1964, Oceanographic aspects of Gulf of California, *in* van Andel, T.H. and Shor, G.G., Jr., eds., Marine Geology of the Gulf of California: American Association of Petroleum Geologists, Memoir 3, p. 30–58.

Roff, J.C. and Legendre, L., 1986, Physico-chemical and biological oceanography of Hudson Bay, *in* Martini, I.P., ed., Canadian Inland Seas: Oceanography Series 44, Elsevier, Amsterdam, p. 265–291.

Rothlisberg, P.C., Pollard, P.C., Nichols, P.D., Moriarty, D.J.W., Forbes, A.M.G., Jackson, C.J. and Vaudrey, D., 1994, Phytoplankton community structure and productivity in relation to the hydrological regime of the Gulf of Carpentaria, Australia, in summer: Australian Journal of Marine and Freshwater Research, v. 45, p. 265–282.

Saleeby, J.B., 1992, Prototectonic and paleogeographic settings of U. S. Cordilleran ophiolites, *in* Burchfiel, B.C., Lipman, P.W. and Zoback, M.L., eds., The Cordilleran Orogen: Conterminous U.S.: The Geology of North America, v. G-3: Geological Society of America, p. 653–682.

Schutter, S.R. and Heckel, P.H., 1985, Missourian (early Late Pennsylvanian) climate in Mid-continent North America: International Journal of Coal Geology, v. 5, p. 111–140.

Scotese, C.R., 1998, Quicktime Computer Animations, PALEOMAP Project: Department of Geology, University of Texas at Arlington, Arlington, Texas. [CD-ROM].

Scranton, M.I., Sayles, F.L., Bacon, M.P. and Brewer, P.G., 1987, Temporal changes in the hydrography and chemistry of the Cariaco Trench: Deep-Sea Research, v. 34, p. 945–963.

Segerstråle, G., 1957, Baltic Sea, *in* Hedgpeth, J.W., ed., Treatise on Marine Ecology and Paleoecology, v. 1: Geological Society of America, Memoir 67, p. 751–803.

Shimkus, K.M. and Trimonis, E.S., 1974, Modern sedimentation in Black Sea, *in* Degens, E.T. and Ross, D.A., eds., Black Sea—Geology, Chemistry, and Biology: American Association of Petroleum Geologists, Memoir 20, p. 249–278.

Smith, R.L., 1992, Coastal upwelling in the modern ocean, *in* Summerhayes, C.P., Prell, W.L. and Emeis, K.-C., eds., Upwelling Systems: Evolution Since the Early Miocene: Geological Society, Special Publication 64, p. 9–28.

Sohlenius, G., Emeis, K-C., Andrén, E., Andrén, T. and Kohly, A., 2001, Development of anoxia during the Holocene fresh brackish water transition in the Baltic Sea: Marine Geology, v. 177, p. 221–242.

Sohlenius, G. and Westman, P., 1998, Salinity and redox alternations in the northwestern Baltic proper during the late Holocene: Boreas, v. 27, p. 101–114.

Somers, I.F. and Long, B.G., 1994, Note on the sediments and hydrology of the Gulf of Carpentaria, Australia: Australian Journal of Marine and Freshwater Research, v. 45, p. 283–291.

Soreghan, G.S. and Giles, K.A., 1999, Amplitudes of Late Pennsylvanian glacioeustasy: Geology, v. 27, p. 255–258.

Soreghan, G.S., Elmore, R.D. and Lewchuk, M.T., 2002, Sedimentologic–magnetic record of western Pangean climate in upper Paleozoic loessite (lower Cutler beds, Utah): Geological Society of America Bulletin, v. 114, p. 1019–1035.

Speed, R.C., Sharp, W.D. and Foland, K.A., 1997, Late Paleozoic granitoid gneisses of northeastern Venezuela and the North America–Gondwana collision zone: Journal of Geology, v. 105, p. 457–470.

Stampfli, G.M., von Raumer, J.F. and Borel, G.D., 2002, Paleozoic evolution of pre-Variscan terranes: from Gondwana to the Variscan collision, *in* Martínez Catalán, J.R., Hatcher, R.D., Arenas, R. and Díaz García, F., eds., Variscan–Appalachian Dynamics: The Building of the Late Paleozoic Basement: Geological Society of America, Special Paper 364, p. 263–280.

Sternbeck, J. and Sohlenius, G., 1997, Authigenic sulfide and carbonate mineral formation in Holocene sediments of the Baltic Sea: Chemical Geology, v. 135, p. 55–73.

Stevenson, G.M. and Baars, D.L., 1986, The Paradox, a pull-apart basin of Pennsylvanian age, *in* Peterson, J.A., ed., Paleotectonics and Sedimentation in the Rocky Mountain Region, United States: American Association of Petroleum Geologists, Memoir 41, p. 513–539.

Struck, U., Emeis, K.-C., Voss, M., Christiansen, C. and Kunzendorf, H., 2000, Records of southern and central Baltic Sea eutrophication in $\delta^{13}C$ and $\delta^{15}N$ of sedimentary organic matter: Marine Geology, v. 164, p. 157–171.

Summerhayes, C.P., Emeis, K.-C., Angel, M.V., Smith, R.L. and Zeitzschel, B., 1995, Upwelling in the ocean: Modern processes and ancient records, *in* Summerhayes, C.P., et al., eds., Upwelling in the Ocean: Modern Processes and Ancient Records: Wiley, Chichester, p. 1–37.

Tomczak, M. and Godfrey, J.S., 1994, Regional Oceanography: An Introduction: Pergamon, Oxford, 422 p.

Torgersen, T., Hutchinson, M.F., Searle, D.E. and Nix, H.A., 1983, General bathymetry of the Gulf of Carpentaria and the Quaternary physiography of Lake Carpentaria: Palaeogeography Palaeoclimatology Palaeoecology, v. 41, p. 207–225.

Torgersen, T., Luly, J., De Deckker, P., Jones, M.R., Searle, D.E., Chivas, A.R. and Ullman, W.J., 1988, Late Quaternary environments of the Carpenteria Basin, Australia: Palaeogeography Palaeoclimatology Palaeoecology, v. 67, p. 245–261.

Trexler, J.H., Snyder,W.S., Cashman, P.H., Gallegos, D.M. and Spinosa, C., 1991, Mississippian through Permian orogenesis in eastern Nevada: Post-Antler pre-Sonoma tectonics of the western Cordillera, *in* Cooper, J.D. and Stevens, C.H., eds., Paleozoic Paleogeography of the Western United States, II: SEPM, Pacific Section, v. 67, p. 317–330.

Walker, D.A., Golonka, J., Ried, A. and Reid, S., 1995, The effects of paleolatitude and paleogeography on carbonate sedimentation in the Late Paleozoic, *in* Huc, A.-Y., ed., Paleogeography, Paleoclimate, and Source Rocks: American Association of Petroleum Geologists, Studies in Geology 40, p. 133–155.

Wallentinus, I., 1991, The Baltic Sea gradient, *in* Mathieson, A.C. and Nienhuis, P.H., Intertidal and Littoral Ecosystems: Elsevier, Amsterdam, p. 83–108.

Wallin, E.T., Noto, R.C. and Gehrels, G.E., 2000, Provenance of the Antelope Mountain Quartzite, Yreka terrane, California: Evidence for large-scale late Paleozoic sinistral displacement along the North American Cordilleran margin and implications for the mid-Paleozoic fringing-arc model, *in* Soreghan, M.J. and Gehrels, G.E., eds., Paleozoic and Triassic Paleogeography and Tectonics of Western Nevada and Northern California: Geological Society of America, Special Paper 347, p. 119–131.

Wasmund, N., 1997, Occurrence of cyanobacterial blooms in the Baltic Sea in relation to environmental conditions: Internationale Revue der gesamten Hydrobiologie, v. 82, p. 169–184.

Watney, W.L., French, J.A., Doveton, J.H., Youle, J.C. and Guy, W.J., 1995, Cycle hierarchy and genetic stratigraphy of Middle and Upper Pennsylvanian strata in the Upper Mid-continent, *in* Hyne, N.J., ed., Sequence Stratigraphy of the Mid-Continent: Tulsa Geological Society, Special Publication 4, p. 141–192.

Wells, M.R., Allison, P.A., Piggott, M.D., Pain, C.C., Hampson, G.J. and De Oliveira, C.R.E., 2005a, Large sea, small tides: the Late Carboniferous seaway of NW Europe: Journal of the Geological Society of London, v. 162, p. 417–420.

Wells, M.R., Allison, P.A., Hampson, G.J., Piggott, M.D. and Pain, C.C., 2005b, Modelling ancient tides: The Upper Carboniferous epicontinental sea of northwest Europe: Sedimentology, v. 52, p. 715–735.

Wignall, P.B., 1994, Black Shales: Clarendon, Oxford, 127 p.

Winfree, K.E., ed., 1998, Cored Reservoir Examples from Upper Pennsylvanian and Lower Permian Carbonate Margins, Slopes and Basinal Sandstones: West Texas Geological Society, Publication 98–103, Midland, Texas, 200 p.

Winkel-Steinberg, N., Backhaus, J.O. and Pohlmann, T., 1992, On the estuarine circulation within the Kattegat, *in* Prandle, D., ed., Dynamics and Exchanges in Estuaries and the Coastal Zone: American Geophysical Union, Coastal and Estuarine Studies 40, p. 231–251.

Winterhalter, B., Flodén, T., Ignatius, H., Axberg, S. and Niemistö, L., 1981, Geology of the Baltic Sea, *in* Voipio, A.V., ed., The Baltic Sea: Oceanography Series 30, Elsevier, Amsterdam, p. 1–121.

Witzke, B.J., 1987, Models for circulation patterns in epicontinental seas applied to Paleozoic facies of North American craton: Paleoceanography, v. 2, p. 229–248.

Wolanski, E. and Ridd, P., 1990, Mixing and trapping in Australian tropical coastal waters, *in* Cheng, R.T., ed., Residual Currents and Long-term Transport: Coastal and Estuarine Studies 38, Springer-Verlag, New York, p. 165–183.

Wolanski, E., 1992, Physical Oceanographic Processes of the Great Barrier Reef: CRC Press, Boca Raton, Florida, 194 p.

Wyrtki, K., 1967, Circulation and water masses in the eastern equatorial Pacific Ocean. International Journal of Oceanography and Limnology, v. 1, p. 117–147.

Yang, K.-M. and Dorobek, S.L., 1995, The Permian Basin of West Texas and New Mexico: Tectonic history of a "composite" foreland basin and its effects on stratigraphic development, *in* Dorobek, S.L. and Ross, G.M., eds., Stratigraphic Evolution of Foreland Basins: SEPM (Society for Sedimentary Geology), Special Publication 52, p. 149–174.

Ye, H., Royden, L., Burchfiel, C. and Schuepbach, M., 1996, Late Paleozoic deformation of interior North America: The greater Ancestral Rocky Mountains: American Association of Petroleum Geologists Bulletin, v. 80, p. 1397–1432.

Ye, H., Royden, L., Burchfiel, C. and Schuepbach, M., 1998, Reply to comments: "Late Paleozoic deformation of interior North America: The greater Ancestral Rocky Mountains": American Association of Petroleum Geologists Bulletin, v. 82, p. 2276–2278.

Youle, J.C., Watney, W.L. and Lambert, L.L., 1994, Stratal hierarchy and sequence stratigraphy—Middle Pennsylvanian, southwestern Kansas, U.S.A., *in* Klein, G.deV., ed., Pangea: Paleoclimate, Tectonics, and Sedimentation During Accretion, Zenith, and Breakup of a Supercontinent: Geological Society of America, Special Paper 288, p. 267–285.

Ziegler, P.A., 1988, Evolution of the Arctic–North Atlantic and the Western Tethys: American Association of Petroleum Geologists, Memoir 43, 198 p.